H. U. SVERDRUP

DYNAMIC OF TIDES ON THE NORTH SIBERIAN SHELF

RESULTS FROM THE MAUD EXPEDITION

DYNAMIC OF TIDES ON THE NORTH SIBERIAN SHELF

RESULTS FROM THE MAUD EXPEDITION

BY

H. U. SVERDRUP

(Received by the Geophysical Commission December 22nd 1926)

Introduction.

The primary object of the present paper is to represent the results of some theoretical investigations which were suggested by observations of the tidal phenomena on the North Siberian shelf during the drift of the «Maud», 1922—1924.

It is generally assumed[1], that the tidal waves, observed on the continental shelves, originate in the adjacent oceans by the action of the tidal forces, but that they proceed across the shelves as free waves under the influence of gravitationel forces only, following the laws which are valid for long, gravitational waves in a resting basin of water. According to these laws the velocity with which the wave proceeds is dependent only on the constant of gravity, g, and the depth of the basin, h. If the depth is uniform the velocity of progress is

$$c = \sqrt{gh} \tag{1}$$

and this formula is supposed to be approximately correct, even when the depth changes, introducing a mean value of h.

The motion of the particles of water is observed as the tidal current and alternates in the direction or against the direction in which the wave proceeds. The greatest velocity in the direction of progress occurs at high water, the greatest velocity in the opposite direction at low water. The currents are uniform from the bottom to the surface.

The tidal phenomena on the continental shelves however, are only exceptionally in agreement with these simple laws. The rate of progress frequently stands not in relation to the depth which is expressed by equation (1) and the tidal currents are generally not alternating but rotating. The deviations from the normal velocity of progress and the occurrence of rotary tidal currents can in some cases be explained as the result of interference between two waves proceeding in different directions, but this explanation appears not always to be possible. This applies, for instance, to the tidal phenomena observed on the North Siberian shelf. All available observations from this region can, as will presently be shown, be united into a picture of a single, progressive wave, entering the shelf from the North, but this picture has little in common with that of a single wave

[1] Otto Krümmel, Handbuch der Ozeanographie, II, p. 238, Stuttgart 1911.

in a resting basin of water, and cannot possibly be obtained as a result of interference between two or more waves of this kind. If, however, we take into consideration the effect of the forces of inertia which arise on account of the rotation of the earth, and the effect of the resistance along the bottom which is transferred to large distances from the bottom on account of the turbulent character of the tidal currents, all the characteristic features can be accounted for.

The influence of the deflecting force of the earth's rotation upon long waves in an infinitely long channel was studied by Lord Kelvin(1). His results are of the highest value to the understanding of some of the features encountered, but they are not sufficient to explain all of them. It has furthermore been suggested by Lord Kelvin, Krümmel(2) and Nansen(3) that rotary tidal currents may result from the action of the deflecting force of the earth's rotation, but an analytical investigation of the character of these currents and the modifications in wave length and wave height by which they may be accompanied, has not been attempted.

The influence of the *viscosity* of the water on the tidal currents close to the bottom has been discussed by Lamb(4). The influence of the *eddy viscosity*, which Lamb recognizes as a factor of importance, has, however, not been the subject of any extensive study.

The results of the present investigations may, as indicated in one of the later chapters, perhaps find a wider application and serve towards a better understanding of some of the irregularities of the tides.

This paper was written and prepared for publication on board the «Maud» during the spring of 1925, when still in the Arctic. This circumstance may serve the author as an excuse for lack of references, particularly to publications which have appeared since 1921.

---

(1) Compare Horace Lamb: Hydrodynamics, Cambridge 1895 p. 334.
(2) l. c. p. 287.
(3) F. Nansen: Spitsbergen Waters, Videnskapsselskapets skrifter 1915 no. 2 p. 86.
(4) l. c. p. 542.

I. The tidal wave on the North Siberian shelf.

1. Observations.

The region which will be dealt with in the present paper, comprises the North Siberian shelf from Point Barrow, Alaska, to Cape Chelyuskin on the Taimir Peninsula, one of the largest continental shelves on the earth.

The geographical distribution of the stations is shown in Fig. 1. The names of the shore stations have been entered and also the numbers of the stations on the shelf. At

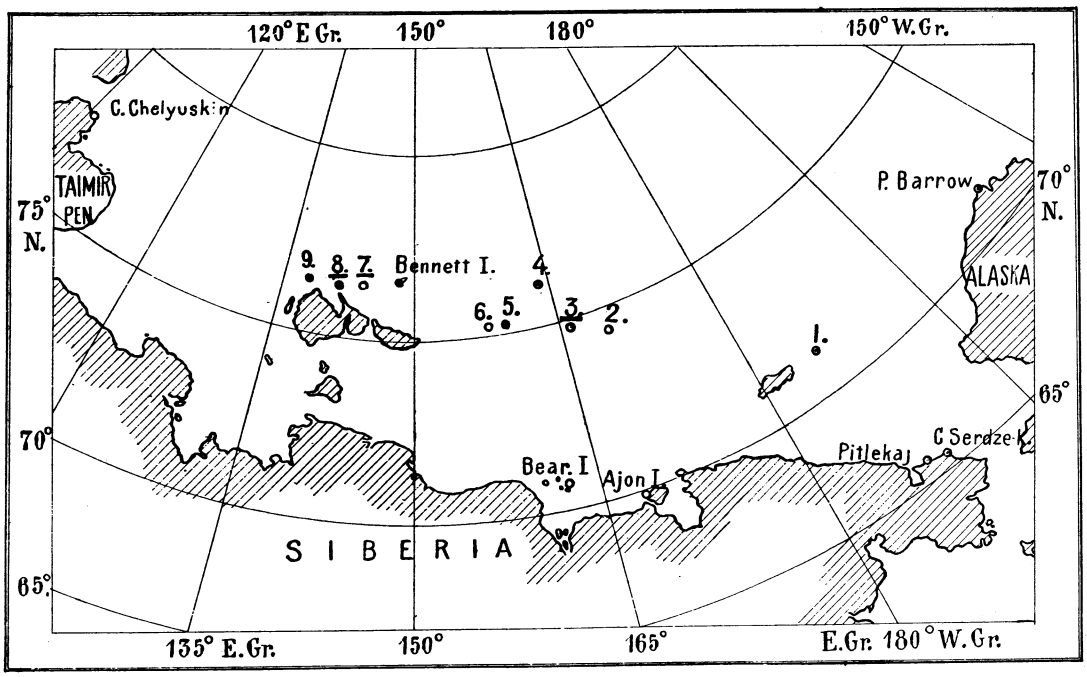

Fig. 1. Geographical distribution of stations.

the major part of the latter only the tidal currents have been observed, at the stations where the number is underlined, the observations have comprised also the range of the tide and the tidal hour.

Tidal observations from this shelf were previously very scarce. When R. A. Harris(1) in 1911 compiled all available tidal observations from the Arctic Regions only 3 stations were situated within the area here mentioned, namely Bennett Island, Pitlekaj and Point Barrow.(2) To these can be added as results from the «Maud»-expedition 4 stations along the Siberian coast, Cape Chelyuskin, Bear Islands, Ajon Island and Cape Serdze-Kamen, where the tides have been registered during intervals covering 6 to 8 months. The last named station is close to Pitlekaj and the two middle stations are not far removed from each other, but neverless give valuable information.

(1) Rollin A. Harris, Arctic tides. Washington 1911.

(2) Harris also gives the tidal hours for two stations at the North-west coast of Alaska (No. 20 p. 56 and No. 1 p. 58, both from B. A. Chart 593) but apparently attaches but little importance to them because he does not refer to them in the text, though one of them decidedly favors his conception of the course of the cotidal lines. Since the information from these stations seems uncertain and is very meager, it will be omitted.

The main data from these stations are entered in Table 1 together with the main data from the three stations which were used by Harris. The data have been condensed in order to make them more comparable with the results of the tidal observations on the open shelf. The latter have to a great extent been made around spring tides, for which reason primarily the conditions at spring will be discussed in the present paper.

The range of the spring tide and the tidal hour at spring are the two quantities, which are of the greatest interest. The tidal hour at spring is closely equal to the number of hours between the culmination of the moon at Greenwich and the Greenwich time of spring high water. At stations with the same tidal hour high water occurs simultaneously. A line joining stations with the same tidal hour, a cotidal line, represents the crest of the tidal ware at this particular hour.

The tidal wave is, however, not regarded as a simple wave but as composed of a series of waves of various period lengths of which the most important are:

Symbol	Period length h
S_2	12.00
M_2	12.42
K_1	23.93
O_1	25.82

At all stations from which tidal observations from a sufficiently long period are available, the semi-ranges and phase angles of these and other components are computed by means of harmonic analysis. The semi-ranges and phase angles and not the spring tide range and tidal hour are generally published. The quality of the tide at any station is characterized by the ratios between the semi-ranges of the components and the differences between the phase-angles. The most important of these quantities are the half-daily index $S_2 : M_2$, the daily index $(K_1 + O_1) : (S_2 + M_2)$ and the age of the spring tide expressed in hours, $0.984\ (S_2^\circ - M_2^\circ)$, where S_2, M_2, K_1 and O_1 mean semi-ranges, and S_2° and M_2° mean phase angles.

From all stations in Table 1 except Bennett Island, harmonic constants are available. At these stations the range of the spring tide has been computed as the double sum of the semi-ranges S_2 and M_2 of the two dominant half-daily waves. This computation is of sufficent accuracy, because the daily index is comparatively small, the tide being mainly half-daily. At Bennett Island the spring range has been computed in assuming the mean semi-range, given by Harris, to correspond to M_2 and the ratio $S_2 : M_2$ equal to 0.4. The tidal hour at spring will not deviate much from the tidal hour of the component M_2, defined by Harris[1] as the phase of this component expressed in lunar hours and increased by the longitude, if this is west and diminished if it is east, the longitude being expressed in hours. The tidal hour of M_2 has, therefore, been entered as «tidal hour at spring» at all stations except Bennett Island, where the mean tidal hour, given by Harris, is used.

The four first columns in Table 1 contain the numbers and names of the stations and their geographical positions. The two next columns contain the spring ranges and tidal hours derived in the described manner, and the last three columns contain a few remarks regarding the quality of the tide at the various stations. This information show that the tide generally has the same character within the entire region. Regarding the data from Bear Islands, the reservation must expressivly be taken that these are preliminary and may be slightly changed by the final editing of the observations.

---

[1] l. c.

Table 1.

No.	Location	Geographical position		Spring tide		$\frac{S_2}{M_2}$	$\frac{K_1+O_1}{M_2+S_2}$	Age of spring tide, days
		Latitude	Longitude	Range cm.	Tidal hour			
		North	West		h			
a	Point Barrow . . .	71° 18′	156° 40′	15	9.65	0.40	0.46	1.6
b	Cape Serdze Kamen	66° 53′	171° 49′	14	6.73	0.70	0.44	—
c	Pitlekaj	67° 03′	173° 30′	7	11.71	0.38	0.73	2.3
			East					
d	Ajon Island. . . .	69° 52′	167° 43′	5	12.33	0.48	0.26	2.0
e	Bear Islands . . .	70° 43′	162° 25′	3	3.2	0.4	0. 6	1.7
f	Bennett Island. . .	76° 41′	149° 05′	105	6.6	—	—	—
g	Cape Chelyuskin. .	77° 33′	105° 40′	34	3.88	0.42	0.40	1.5

a c f Rollin H. Harris; Arctic Tides, Washington 1911.
b o g J. E. Fjeldstad: Litt om tidevandet i Nordishavet. Naturen V. 47. Bergen 1913.
e Preliminary values from registrations October 1924 to April 1925.

This reservation must also be taken regarding the preliminary results of the tidal observations on the open shelf, which were carried out during the drift of the «Maud» along the North Siberian shelf in 1922—1924. These observations comprise several series of hourly soundings by means of which the range of the tide and the time of highwater were determined directly. Furthermore, they comprise a great number of current measurements, partly accomplished by means of a selfrecording currentmeter, which was designed and constructed on board the «Maud» and kept in operation in various depths during the major part of 14 months, from March 1923 to April 1924, partly by means of Ekman's currentmeter, used in various depths during at least 13 hours at the stations from which the preliminary results are published in this paper. All current measurements were carried out from the drifting ice and therefore could only give the motion of the water relatively to the motion of the ice. In order to te find the absolute currents, the drift of the ice had to be determined independently. This was accomplished by letting a lead run down to the bottom with so great speed that at stuck, and then noting the length of wire which was hauled out in a sertain number of minutes, and the direction in which the wire was running out. By means of the data an the knowledge of the depth the velocity and the direction of the drift of the ice could be computed. This method, which was used by Nansen[1], gave, judging from the close agreement between the values obtained by different observers, reliable results, when the ice was relatively scattered, making it possible to observe accurately the direction, in which the wire was running out, and could even when only a narrow hole in the ice was at hand be used to ascertain whether a considerable tidal movement of the ice took place or not.

In Table 2 the main results of the direct soundings are compiled. By the derivation of the represented results only the soundings made around spring tide have been utilized because they evidently must be expected to give the most reliable results, but it has been ascertained that all observations from the same regions rendered practically the same tidal interval. The soundings were so treated that the depth was determined for every lunar hour, reckoned from the transit of the moon across the local meridian at full or change, by means of graphical interpolation between the observed depths. These values were at each station united to means, and the range of the tide and the lunitidal interval, expressed in lunar hours, computed by harmonic analysis. The tidal hours

(1) l. c.

at spring were finally obtained by subtracting the east longitudes expressed in hours from the lunitidal intervals. The ranges and tidal hours at spring are to be found in the Table in the 6th and 7th columns and the dates of the nearest full or new moon are entered under

Table 2. Preliminary results of soundings.

No.	Date	Number of half-day periods	Geographical position		Spring tide		Remark
			Latitude North	Longitude East Gr.	Range cm	Tidal hour	
3	Apr. 30—May 4, 1923	8	74° 41′	166° 25′	18	8.2	Full moon May 1.
7	July 2—5 1924. . .	7	76° 30′	144° 00′	92	5.4	New moon July 2.
8	July 18—20 1924. .	2	76° 30′	141° 40′	210	5.0	Full moon July 16.

remarks. These results can naturally not claim a high degree of accuracy, partly because they were made, while the ship was drifting with the ice over a more or less uneven bottom. There is neverless, an astonishing good agreement between the results of the soundings and of the current measurements.

The current measurements can be devided into two groups, one containing measurements which were made at a depth, were the strongest currents were found, and continued during long periods and the other containing measurements made at various depths during at least 13 hours in order to determine the variations of the tidal currents with depth and the mean tidal currents from the bottom to the surface. The latter were generally carried out around spring tide, when the greatest velocities could be expected.

The observed currents have been treated in a similar way as the observed depths. The currents were decomposed into a North and an East component and for each component the amplitude and the lunitidal interval of maximum value, expressed in lunar hours, was computed in the way used when dealing with the soundings. The components could always be closely represented by a single harmonic term. They were again united, and the directions and velocities of maximum and minimum current as well as the lunitidal interval of maximum current, determined. By adding the west or subtracting the east longitudes there was derived finally, what may be called «tidal hour of maximum current». The current was found to be rotary at all stations. The direction of rotation will at each station be described as clockwise, cl. or counter clockwise, c.cl.

The main results are compiled in Table 3. The first part of the table contains the results from 4 stations, at which the currents were observed in one or two depths only, the last part contains the results from 5 stations at which measurements were made in a sufficient number of depths to allow a determination of the mean tidal currents from the bottom to the surface. The contents of the Table are fully explained by the headlines and the preceding information regarding the metods by which the various values have been derived.

The tidal currents were never found to be uniform from the bottom to the surface. The variations with depth were different at the various stations. One example may in this place illustrate the complicated character of the currents. Table 4 contains the result of registration during May 17 to 20 and May 29 to June 2, 1923. From this Table it is seen that the ice and the upper 30 meters of the sea took practically no part in the tidal movement. Between 40 and 45 meters strong tidal currents were encountered, rotating clockwise and running with practically the same velocity in all directions.

Table 3. *Preliminary results of current measurements.*

No.	Date	Geographical positions		Depth m.	Depth in which tidal current measured m.	Max tidal current			Min. tidal current cm./sec.	Ratio $\frac{\text{Min.}}{\text{Max.}}$	Dir. of rot.	Full or new moon
		Lat. North	Long. West			cm./sec.	Against (true direction)	Tidal hour				
1	Aug. 8—10 1922 . .	71° 20′	175° 00′ East	76	0, 20	16.5	S	9.5	13.0	0.79	cl.	Aug. 7
2	March 20—21 1923 .	74° 11′	169° 45′	50	40	20.0	S 45° W	8.4	18.0	0.90	cl.	March 18
5	Nov 24—27 1923 .	75° 12′	159° 40′	38	28	9.5	S 55° W	9.1	7.5	0.78	cl.	Nov. 23
6	Febr. 6—9 1924 . .	75° 11′	157° 40′	38	28	9.5	S 55° W	8.9	5.0	0.58	cl.	Febr. 5
3	May 17—20 and May 29—June 2. 1923	74° 40′	166° 10′	56	0—56	3.8	S 55° W	8.2	3.0	0.79	cl.	May 16 May 29
4	Aug. 27—Sept. 2. 1923	76° 10′	164° 00′	64	0—64	6.5	S 15° W	7.5	4.2	0.65	cl.	Aug. 25
7	June 30 and July 3. 1924	76° 32′	144° 00′	35	0—35	16.5	S 10° E	4.8	5.5	0 33	cl.	July 2
8	July 18. 1924 , . .	76° 28′	141° 30′	22	0—22	38.0	S 45° E	3.0	5.0	0.13	cl.	July 16
9	August 1. 1924 . .	76° 36′	138° 30′	22	0—22	22.5	S 50° E	2.2	13.0	0.58	cl.	Aug. 1

Table 4. *Preliminary results of current measurements at station 3. North. Lat. 74° 40′ East Long. 166° 10′ Depth 56 m. May 17—20 and May 29 to June 2 1923.*

Depth m.	Max tidal current			Min. tidal current cm./sec.	Ratio $\frac{\text{Min.}}{\text{Max}}$	Direction of rotation	Number of half-day periods	Remarks
	cm./sec.	Against (true)	Tidal hour					
0—30								To weak to be observed.
35	6.2	S 50° W	8,9	5.4	0.87	cl.	4	
42	15.4	S 73° W	8.9	12.9	0.84	cl.	4	
46	11.0	S 29° W	7.2	8.8	0.80	cl.	2	
50	5.4	N 87° W	6.8	2.8	0.52	cl.	4	

The velocities decreased again rapidly when approaching the bottom, and the greatest velocities occurred there earlier than above. At the greatest depth in which the tidal currents were registred, 50 meters, the direction of maximum velocity deviated furthermore towards the right of the corresponding direction in greater distances from the bottom, and the ratio between minimum and maximum velocity was smaller.

Finally a few data regarding the quality of the tides may be derived from the current observations. If the maximum velocity of the tidal current in a constant depth is plotted as a function of time, it is found to vary regularly during 14 days. The greatest value u_s evidently occurs at spring and the smalled u_r at neap tide. Assuming that the tidal currents are proportional to the semi-range of the tidal wave, and that this at spring tide is equal to the sum of the semi-ranges of the two most important halfday-tides M_2 and S_2 and at neap equal to the difference between these semi-ranges, we obtain

$$\frac{u_s}{u_r} = \frac{M_2 + S_2}{M_2 - S_2}$$

By means of this relation the half-day-index $S_2 : M_2$ can be derived, if current observations from any depth are available for a sufficiently long period. The time-difference

between full (or new) moon and the occurrence of the strongest tidal currents will evidently render an approximate value of the age of the spring tide.

Table 5 contains a few values of the half daily index and the age of the spring tide which have been derived in this way.

No conspicous daily variation of the currents has been observed.

Table 5. *Preliminary results regarding the quality of the tide.*

Period	Geographical position		$\frac{S_2}{M_2}$	Age of spring-tide. Days
	Lat. North	Long. East		
March 1923	74° 10′	169°	0.35	2.7
August 1923	76° 00′	164°	0.5	2.5
June 1924	76° 30′	144°	0.4	2.7

2. Representation of results.

We shall at first turn to the results of the current measurements. In Fig. 2 the direction of the maximum currents at spring are plotted as arrows and the corresponding tidal hours entered. The hours are written in Roman figures, the decimal fraction of the hours in Arabic figures. The character of the tidal currents is indicated by ellipses. The ratio between the axes of these is equal to the ratio between minimum and maximum current, and the direction in which the current rotates is indicated by arrow heads. At stations where the mean tidal currents from the bottom to the surface have been determined, the ellipses are fully drawn; where the observations have been limited to one or two depths, they are stippled.

The most striking feature in this representation is, that the tidal currents rotate clockwise at *all* stations. The fact that the direction of rotation is the same at all stations, provides the strongest evidence that these currents cannot result from interference between two simple waves, propagating in different directions, because the phasedifference between two such waves must vary from place to place and according to the phasedifference under which the waves meet, regions with clockwise rotating currents must alternate with regions with counterclockwise rotating currents. In order to demonstrate this by an example Fig. 3 has been prepared. It is here supposed, that the rotary currents in latitude 75° North and longitude 165° East are produced by interference between two waves of equal height but with a phase difference of 3 hours, one proceeding from NE towards SW with tidal hour VIII at the place mentioned, and one proceeding from NW towards SE with tidal hour V. The depth of the sea for sake of simplicity is supposed to be uniform and equal to 50 meters according to which both waves progress with a velocity of 22 m./sec. The coastline has been drawn as a fine dotted line to facilitate comparison with Fig. 2, and simultaneously to indicate that Fig. 3 does not represent an actual map of the regions in question. The fine lines runing NW—SE and NE—SW marked in the Roman figures, represent the cotidal lines of the two waves corresponding to the supposed velocity of progress. The directions are here referred to meridian 165° E. From the cotidal lines it is seen, that the phasedifference between the two waves is zero along the vertical lines marked N. Along these lines, therefore, the tidal currents must run alternately South or North. Along the lines marked E the

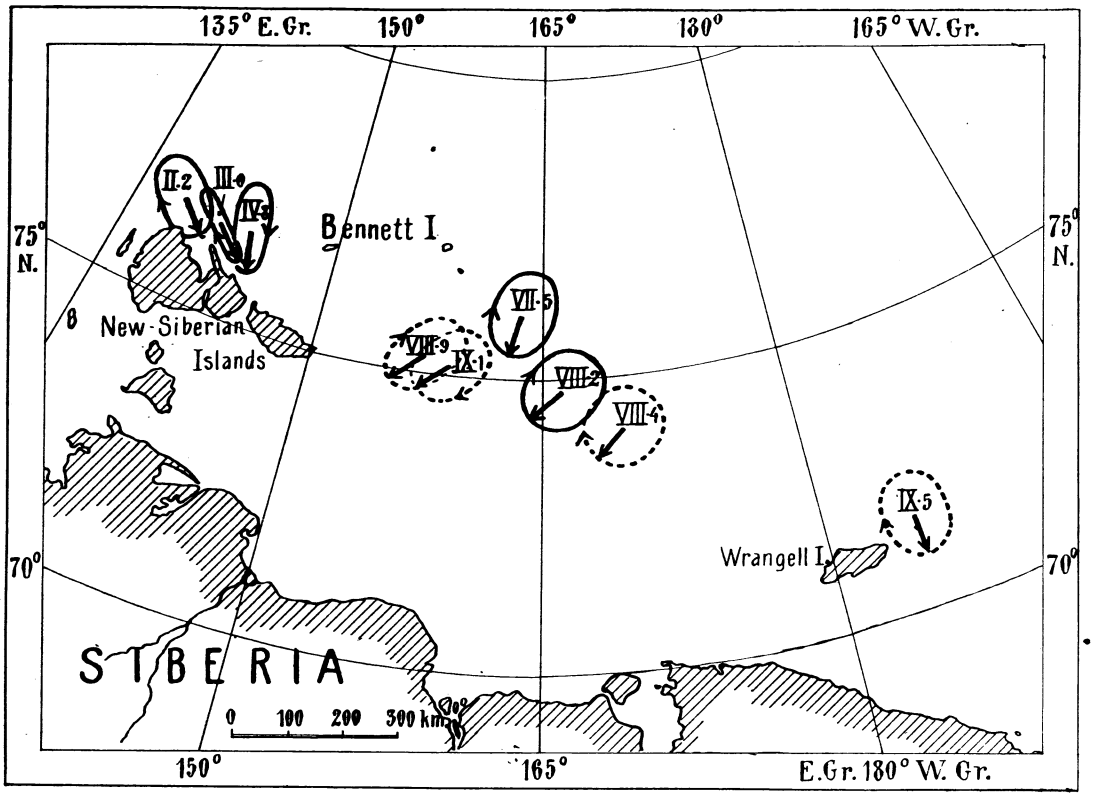

Fig 2. Tidal currents on the North-Siberian shelf.

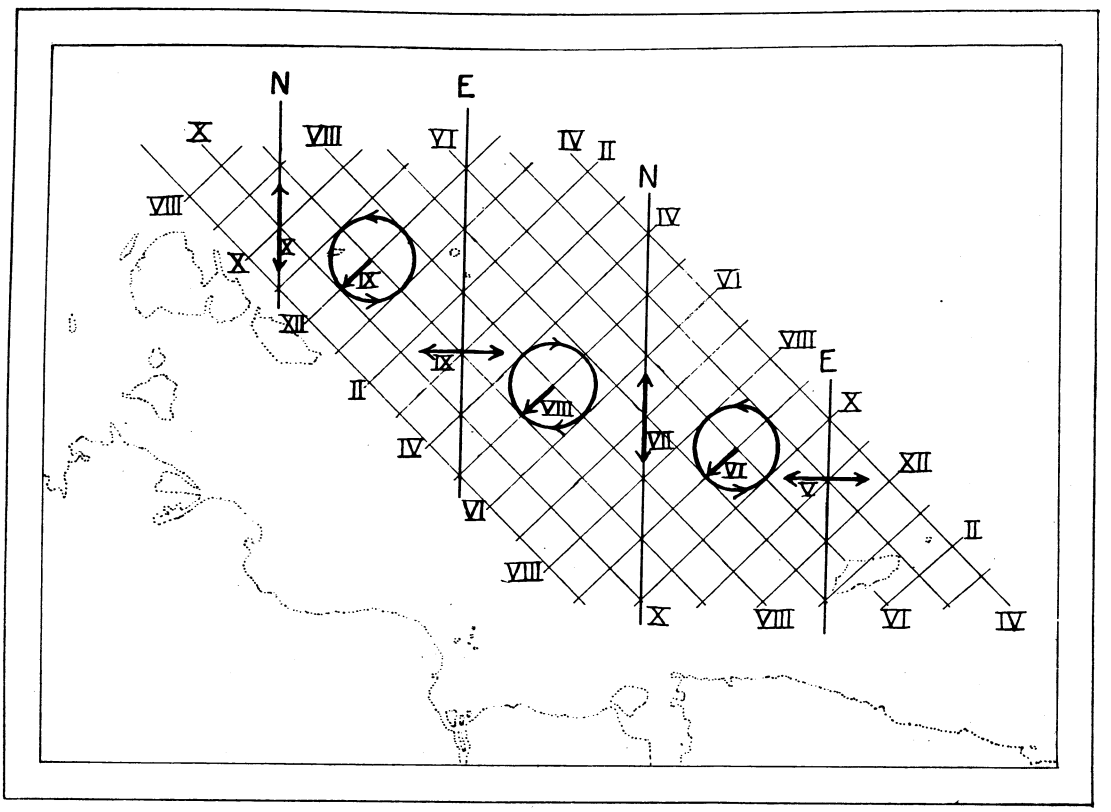

Fig. 3. System of tidal-currents resulting from interference between two waves.

difference in phase is 6 hours, and the currents run alternately West or East. In the regions between the lines N and E the currents rotate counter clockwise, in the regions between E and N clockwise, as indicated by the arrow heads on the circles which represent the character of the tidal currents in the central parts of these regions. The direction of the maximum tidal current changes within the regions between the lines N and E, from South over SW to West and turns between E and N back again from West to South.

A comparison between the two figures shows that the constructed currents are far more complicated than those observed. Attention may for instance be drawn to the central parts of the figures, where the actual depth varies between 60 and 40 meters, thus corresponding well to the supposed depth of 50 meters. If the clockwise rotating currents in latitude 75° N and long. 165° E resulted from the supposed interference, we should according to Fig. 3 have observed alternating currents running North—South for a distance of 165 km. to the east of the place mentioned, and alternating currents running East—West proceeding 165 km. to the west but we have in both distances observed currents which rotated clockwise with maximum current towards practically the same direction. Other attempts to explain the rotary currents by interference have failed in the same way, even if the progressions of the asumed waves have been brought in accordance with the actual depths. It is always possible to choose one pair of interfering waves so that the observed conditions at one station can be explained, but every selection of waves involves consequenses which are in striking disagreement with the conditions at other stations. From this inspection of the tidal currents alone we are therefore led to suppose that the tidal phenomena on the North Siberian shelf are created by one tidal wave. It will be shown later that the rotary character of the currents can be explained in a satisfactory way as the result of the action of the deflecting force of the earth's rotation.

The simplest assumptions which in this place can be made regarding the relations between the rotary tidal currents and the tidal wave, appear to be, that the tidal currents reach their greatest velocity at high-water and that at that time they run in the direction in which the wave proceeds. The cotidal lines of the wave must be based upon all available observations and according to the above assumptions be so drawn that they:

1. agree with the observed tidal hours and «tidal hours of maximum currents»
2. run perpendicularly to the directions of the maximum currents.

In Fig. 4 all the main data contained in Tables 1 to 3 have been entered. The depth of the sea is indicated by stippled isobaths for 25, 50, 75 and 100 meters, which are based upon the soundings entered on the hydrographic charts of the Arctic Sea, published by the United States Coast and Geodetic Survey and the Russian Hydrographic Office, the latter containing the results from the expeditions with the ice-breakers «Taimir» and «Vaigach», 1912 and 1913, and the soundings taken during the drift of the «Maud» The lines marked with Roman figures represent the cotidal lines which have been drawn according to the stated principles. An inspection shows, that these lines unite all observations into a simple and consistent picture. In the region North of the New-Siberian Islands there is a discrepancy between the time of maximum current and the time of high-water and the cotidal lines have here been made to agree with the time of high-water. Otherwise the mutual agreement between the various observations is evidently very good.

The cotidal lines have a marked tendency to run parallel to the isobaths. The tidal wave appears to enter the shelf from the North and to reach the region, northeast of Cape Chelyuskin and north of the New-Siberian Islands at first. The observations from

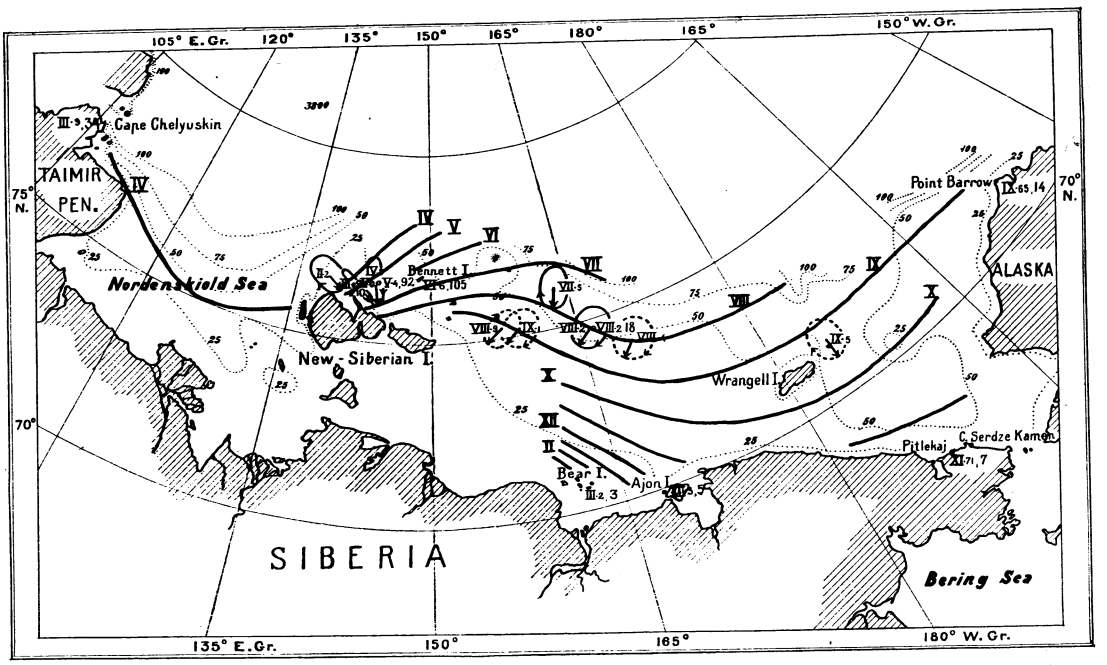

Fig. 4.

the latter region can hardly be united with the observation at Cape Chelyuskin otherwise than by drawing the cotidal line IV in a great curve towards the south. This curve seems to correspond closely to the bay which the deep ocean forms in the northern part of Nordenskiold Sea, indicating that the wave travels so rapidly in this deep water, that it reaches the most northerly part of the shelf and the bottom of the deep-water bay almost simultaneously. The 100 meters isobath actually represents in this region according to the soundings made by the «Taimir» and «Vaigach» the border of the continental shelf. In the regions northwest and east of Wrangell Island the cotidal lines have the same tendency to follow the isobaths, indicating that the wave proceeds with a greater speed due north of Wrangell Island than on the shelf northwest of this island. The available soundings in this region show a marked increase in the depth towards north, but whether this increase indicates the border of the continental shelf or not is an open question.

The observations at Cape Serdze Kamen have been disregarded, because the conditions there are evidently complicated by a tidal wave entering through Bering Strait.

The course of the cotidal lines to which we here have arrived, differs entirely from the course of the cotidal lines on the same shelf that were plotted by Rollin A. Harris in 1911(1). Harris, however, based his result for this region mainly on three stations Bennett Island, Pitlekaj and Point Barrow. He was led to the conclusion that the tidal wave proceeds from Bennett Island to Point Barrow in a practically East—Westerly direction, and that this course was necessitated by the existence of extensive masses of land or shoals within the still unknown region of the Arctic territory.

J. E. Fjeldstad(2) in 1923 drew new cotidal lines for the Arctic Region, utilizing the registrations from the stations Cape Chelyuskin and Ajon Island of the «Maud»-Expedition. He finds, in agreement with the results represented in this paper, that the tidal wave enters the North-Siberian shelf from the North, and concludes that the wave travels

(1) L. c.
(2) Litt om tidevandet i Nordishavet, Naturen V. 47. 1923 p. 161—175.

directly across the Arctic Sea from the Spitsbergen—Greenland opening to Alaska, without meeting obstructions formed by extensive masses of land. That the tidal wave enters the shelf from the North is in agreement with the results represented in this paper. It seems therefore, justifiable to conclude that the tidal phenomena do not indicate the existence of land within the unexplored area. Fjeldstads cotidal lines on the shelf itself differ, however, considerably from the lines drawn in Fig. 4. It seems unnecessary to enter upon the differences, because the new cotidal lines are based upon far more extensive observations than those previously available. Particular attention may be drawn to the observations from Ajon Island and Bear Islands, because the circumstance that the tidal wave arrives 3 hours later at the Bear Islands than at Ajon Island agrees perfectly with the conclusions regarding the direction of progress of the wave in this region which were actually drawn from the current observations on the shelf before the registrations at the Bear Islands had been carried out(1).

The picture of the tidal wave on the North-Siberian shelf to which we have here arrived, is comparatively simple and unites as already emphasized all observations in a satisfactory way. It may in this connection be mentioned, that the practically uniform quality of the tide within the whole region (Tables 1 and 5) supports the conception, that we have a single tidal wave before us. The result has, however, very little in common with the picture of a long wave which proceeds in a non-viscous fluid on a resting basin under the influence of gravitational forces only. We shall draw attention to the main points on which the observed conditions disagree with those which should have been expected, if the wave had been of the above mentioned, simple kind.

1. The tidal currents do not run alternately in the direction in which the wave proceeds or against this direction, but within the whole region rotate clockwise. At great distances from the shores the difference between the strongest and weakest currents is very small, but directly north of the New-Siberian Islands approximately alternating currents are found at the stations which are nearest to these islands.

2. The tidal currents are not uniform from the bottom to the surface but the phase and the direction of maximum current as well as the ratio between the minimum and maximum velocities vary with the depth.

3. The time of maximum current does not correspond exactly to the time of high water. This applies particularly to the region north of the New-Siberian Islands, where the tidal currents reach their greatest velocities 1 to 2 hours before high water.

4. The velocity with which the wave proceeds differs considerably from the value computed by means of the simple equation:

$$c = \sqrt{gh}.$$

Where the currents run with approximately the same velocity on all directions the wave proceeds too fast, and where the currents are approximately alternating, too slowly. South of Station 1, for instance, the average depth is approximately 55 meters, giving a computed velocity of progress:

$c = \sqrt{gh} = 23{,}2$ m./sec. as compared with 65 m./sec observed and south of Station 3 the average depts is about 50 meters giving:

$c = \sqrt{gh} = 22.1$ m./sec. as compared to 27 m./sec. observed. At Station 8 on the other hand the velocity of progress corresponding to a depth of 22 meters is

$c = \sqrt{gh} = 14.7$ m./sec. as compared with 10 m./sec. observed.

(1) Radiogram to Norwegian Newspapers, f. i. Aftenposten. Dec. 4. 1923.

5. The range of the tides varies within wide limits, from 210 cm. at Station 8 to only 3 cm. at Bear Islands. A closer inspection reveals that the range decreases both along the wave front, represented by the cotidal lines, and in the direction in which the wave proceeds. The decrease of the range along the wave front is particularly conspicous between the New-Siberian Islands and Point Barrow, where the observed values are 210 cm. and 14 cm. respectively. Referred to the direction in which the wave proceeds the decrease takes place from the right side of the wave to the left side. The decrease in the direction of progress is evident from the observations at Station 3, Ajon Island and Bear Island, where the respective ranges are 18, 5 and 3 cm., and from the observations at Point Barrow and Pitlekaj where the ranges are 14 and 7 cm. These variations cannot be accounted for if the above mentioned simple assumptions regarding the character of the wave are maintained.

6. The quality of the tide shows small, but irregular variations within the region

All these characteristic features lead to the conclusion, that it is not sufficient to assume, that the tidal wave proceeds under the influence of gravitational forces only. It seems necessary to take into account the effect of the deflecting force of the earth's rotation as well as the effect of the resistance, which is magnified by the turbulent character of the tidal currents. This consideration suggested the investigation of long gravitational waves on a rotating disc and of the influence of the eddy-viscosity on such waves. The results show that all the characteristic features which have been pointed out here, can be satisfactory explained, and confirm the view that the cotidal lines, ranges and tidal currents, which are represented in Fig. 4, together give an approximately correct picture of the tidal phenomena on the North-Siberian shelf at spring tide.

The reader who does not wish to enter upon the mathematical developments of the following chapters may turn to Chapter 15 p. 55 where the theoretical results have been summarized.

II. Long gravitational waves in a non-viscous, homogeneous fluid.

3. Waves in a resting basin.

In the following only long, proceeding, gravitational, plane waves will be dealt with, meaning long waves proceeding under the influence of gravitational and inertia forces only and with a straight wave front. We shall at first suppose the fluid to be non-viscous and the motion free of turbulence, and may, therefore, base the considerations upon the treatment of long waves in a rotating fluid which is given by Lamb(1). It may, however, be of advantage to remember the equations for long, plane waves in a fluid in a resting basin(2).

We shall suppose the fluid layer to be unlimited and of even depth. The x-axis shall be horizontal, coincide with the direction in which the wave proceeds, the z-axis vertical and positive upwards. The ordinate of the free surface, which at the time t corresponds to the abscissa x will be denoted by.

$$z_0 + \zeta$$

where z_0 means the ordinate, when the conditions are undisturbed.

Since we are dealing with long waves only, we can place the vertical accelerations out of consideration and regard the pressure at any point x, z as identical with the statical pressure corresponding to the distance from the free surface, or:

$$p - p_0 = g\varrho\,(z_0 + \zeta - z), \tag{1}$$

where p_0 is the constant pressure at the free surface, g the acceleration of gravity and ϱ the constant density.

Of (1) we find:

$$\frac{\partial p}{\partial x} = g\varrho\,\frac{\partial \zeta}{\partial x} \tag{2}$$

The equation for the horizontal motion of fluid particles, since external forces are excluded, has the form:

$$\frac{Du}{Dt} = \frac{\partial u}{\partial t} + u\,\frac{\partial u}{\partial x} = -\frac{1}{\varrho}\,\frac{\partial p}{\partial x}, \tag{3}$$

where u is the velocity in the direction of the x-axis. This equation in the present case is simplified, because the term $u\,\frac{\partial u}{\partial x}$, when dealing with long waves, is small of second order, and can be omitted. We, therefore, find:

$$\frac{\partial u}{\partial t} = -g\,\frac{\partial \zeta}{\partial x}. \tag{4}$$

The equation of continuity can be written:

$$\frac{\partial u}{\partial x} + \frac{\partial w}{\partial z} = 0, \tag{5}$$

(1) L. c. p. 331.
(2) Lamb, l. c. p. 271.

where w means the velocity along the z-axis. From this equation, since the depth is supposed to be constant, we obtain:

$$w = -\int_0^z \frac{\partial u}{\partial x} dz = -h \frac{\partial u}{\partial x}, \tag{6}$$

where h denotes the depth. At the free surface:

$$z = h + \zeta \quad \text{and} \quad w = \frac{\partial \zeta}{\partial t},$$

and we therefore find:

$$\frac{\partial \zeta}{\partial t} = -h \frac{\partial u}{\partial x}. \tag{7}$$

The equations (4) and (7) determine the motion of the fluid particles and the velocity of progress of the wave.

The deformation of the free surface may be represented by the equation

$$\zeta = \zeta_0 \sin 2\pi \left(\frac{t}{T} - \frac{x}{L} \right) \tag{8}$$

If the deformation is of a more complicated character, it can always be represented by a sum of terms of this form, but for sake of simplicity we will suppose that a single term in sufficient. Equation (8) represents a wave proceeding an the direction of the positive x-axis with the velocity:

$$c = \frac{L}{T}, \tag{9}$$

where T is the period length and L the wave length. We shall introduce:

$$\sigma = \frac{2\pi}{T} \quad \text{and} \quad \mu = \frac{2\pi}{L}, \tag{10}$$

where σ is the frequens of the wave. Equation (8) can then be written:

$$\zeta = \zeta_0 \sin (\sigma t - \mu x) \tag{11}$$

Introducing the value of ζ in (4) and integrating we find:

$$u = g \frac{\zeta_0}{c} \sin (\sigma t - \mu x). \tag{12}$$

From equations (7) and (12) we get:

$$\zeta = g \frac{h \zeta_0}{c^2} \sin (\sigma t - \mu x),$$

but this equation must be identical with (11), giving:

$$c = \sqrt{gh}. \tag{13}$$

The velocity of progress thus depends only upon the depth, h.

A comparison between equations (11) and (12) shows that the velocity reaches the greatest positive value, i. e. the greatest value in the direction of progress, when the wave height is greatest and the max. velocity is:

$$u_{max} = g\frac{\zeta_0}{c} = c\cdot\frac{\zeta_0}{h} = \sqrt{\frac{g}{h}}\cdot\zeta_0 . \tag{14}$$

The horizontal motion of the fluidparticles is furthermore independent of z; uniform from the bottom to the free surface.

Finally we shall compute the mean energy during one period of a column of fluid with square section equal to the square unit. The potential energy due to an upheaval or lowering of the free surface above or below the mean level is for $x = x_0$ and $t = t_0$:

$$E_p = g\varrho\int_0^{\zeta} z\,dz = \frac{1}{2}g\varrho\zeta^2 ,$$

and the mean during one period is:

$$\bar{E}_p = \frac{1}{2}g\varrho\frac{1}{T}\int_0^T \zeta^2\,dt = \frac{1}{4}g\varrho\zeta_0^2 . \tag{15}$$

The corresponding mean kinetic energy is:

$$\bar{E}_k = \varrho\frac{1}{T}\int_0^h\int_0^T \frac{1}{2}u^2\,dz\,dt = \frac{1}{4}g\varrho\zeta_0^2 . \tag{16}$$

The total mean energy is

$$\bar{E} = \bar{E}_p + \bar{E}_k = \frac{1}{2}g\varrho\zeta_0^2 \tag{17}$$

of which one half is potential and the other half kinetic. Since the mean energy depends only upon the amplitude of the wave it seems justifiable to conclude that the amplitude remains unchanged, if the depth changes in the direction of progress, but the conclusion is evidently only an approximation because all equations are based upon the assumption that the depth is constant.

4. Long, gravitational waves in a rotating fluid.

We will next turn to waves in a fluid layer of even depth, rotating around a vertical axis. The results may without great restrictions be applied to waves within a region of not too large dimension on a rotating sphere.

The axis of rotation shall be taken as z-axis, and the x- and y-axes are supposed to rotate in their plane with the given angular velocity ω. The velocities of the fluid particles relatively to these axes will be called u, v and w. The real velocities parallel to the same axes are then:

$$u - \omega y \quad , \quad v + \omega x \quad , \quad w$$

and the accelerations:

$$\frac{Du}{Dt} - 2\omega v - \omega^2 x \quad , \quad \frac{Dv}{Dt} + 2\omega u - \omega^2 y \quad , \quad \frac{Dw}{Dt} .$$

The ordinate of the free surface, when the latter is in equilibrium under the influence of the gravitational and centrifugal forces, may be called z_0, We then have:

$$z_0 = \frac{1}{2}\frac{\omega^2}{g}(x^2 + y^2) + \text{const.} \tag{1}$$

It shall be supposed, that the inclination of this surface is small, which means that $\frac{\omega^2}{g} r$ is a small quantity, where r is the distance from the axis of rotation.

If the ordinate of the deformed surface is called $z_0 + \zeta$, the pressure in any point x, y, z is defined by:

$$p - p_0 = g\varrho\,(z_0 + \zeta - z), \tag{2}$$

supposing as previously that the vertical accelerations can be omitted. From (2) we find:

$$-\frac{1}{\varrho}\frac{\partial p}{\partial x} = -\omega^2 x - g\frac{\partial \zeta}{\partial x}$$
$$-\frac{1}{\varrho}\frac{\partial p}{\partial y} = -\omega^2 y - g\frac{\partial \zeta}{\partial y}.$$

Assuming as previously, that $\frac{D}{Dt}$ can be replaced by $\frac{\partial}{\partial t}$, we finally get the equations for the horizontal velocities in the form:

$$\begin{aligned} \frac{\partial u}{\partial t} - 2\omega v &= -g\frac{\partial \zeta}{\partial x} \\ \frac{\partial v}{\partial t} + 2\omega u &= -g\frac{\partial \zeta}{\partial y}. \end{aligned} \tag{3}$$

If ω represents the velocity of rotation of the earth equations (3) can be applied to waves in a basin of not too great dimensions at the poles. If the equations are to be applied to waves in a basin in the latitude φ the vertical component of the velocity of rotation:

$$\omega' = \omega \sin \varphi$$

must be introduced in equations (3). We shall therefore, with future applications in view, write equations (3) in the form:

$$\begin{aligned} \frac{\partial u}{\partial t} - \lambda v &= -g\frac{\partial \zeta}{\partial x} \\ \frac{\partial v}{\partial t} + \lambda u &= -g\frac{\partial \zeta}{\partial y}, \end{aligned} \tag{4}$$

where λ now means the double angular velocity of rotation of the disc, but where we shall later introduce:

$$\lambda = 2\omega \sin \varphi,$$

where ω means the angular velocity of rotation of the earth.

The equation of continuity can be written (eq. (5) to (7) of Chapter 3):

$$\frac{\partial \zeta}{\partial t} = -h\frac{\partial u}{\partial x} - h\frac{\partial v}{\partial y}, \tag{5}$$

where h means the constant depth. This is evidently constant only when the bottom has the same curvature as the free surface, defined by equation (1).

The following investigation is based upon equations (4) and (5), which can be integrated in a few special cases.

5. Waves in an infinitely long, straight rotating channel.

Lord Kelvin has shown, that in an infinitely long, straight channel the equations (4) and (5) are satisfied by the values:

$$\begin{aligned} \zeta &= \zeta_0 e^{-\frac{\lambda}{c} y} \sin(\sigma t - \mu x) \\ v &= 0 , \end{aligned} \tag{1}$$

when the x-axis is parallel to the direction of the channel. Substituting these values in (4) Chapter 4 we find:

$$u = g \frac{\zeta_0}{c} e^{-\frac{\lambda}{c} y} \sin(\sigma t - \mu x) \tag{2}$$

and from the equation of continuity:

$$c = \sqrt{gh} . \tag{3}$$

According to the last equation the velocity of progress is not influenced by the rotation.

The exponential factor in equations (1) and (2) shows, that the amplitude of the wave and the horizontal velocities decrease from one side of the channel to the other. If the rotation is positive, i. e. takes places from the positive x-axis to the positive y-axis, the amplitude decreases from right to left referred to an observer looking in the direction of progress, if negative from left to right. If the breadth of the channel is called b the amplitudes at both sides are respectively:

$$\zeta_0 \quad \text{and} \quad \zeta_0 e^{-\frac{\lambda}{c} b} .$$

For a numerical example we may select $\lambda = 1.456.10^{-4} =$ the double angular velocity of the earth's rotation, $g = 9.82$ m. sec.$^{-2}$, $h = 50$ m. giving $c = 22.1$ m. sec.$^{-1}$. We then find the following relative values for varions values of b:

b km.	ζ_0	$\zeta_0 e^{-\frac{\lambda}{c} b}$
10	1.0	0.94
100	1.0	0.51
1000	1.0	0.002

The maximum horizontal velocities along the two sides of the channel stand in the same ratio as the amplitudes. For an increasing breadth of the channel the wave seems to proceed practically along only one side of the channel.

6. Waves on an unlimited, rotating disc.

On an unlimited rotating disc the equations (4) and (5) of Chapter 4 are satisfied by:

$$\begin{aligned} \zeta &= \zeta_0 \sin(\sigma t - \mu x) \\ \frac{\partial v}{\partial y} &= 0 \end{aligned} \tag{1}$$

Equations (4) and (5) are reduced to:

$$\begin{aligned} \frac{\partial u}{\partial t} - \lambda v &= g\,\zeta_0 \cos(\sigma t - \mu x) \\ \frac{\partial v}{\partial t} + \lambda u &= 0 \end{aligned} \tag{2}$$

and

$$\frac{\partial \zeta}{\partial t} = -h\frac{\partial u}{\partial x}. \tag{3}$$

Of (2) we find:

$$\begin{aligned} u &= \frac{g}{c}\zeta_0 \frac{\sigma^2}{\sigma^2 - \lambda^2}\sin(\sigma t - \mu x) \\ v &= \frac{\lambda}{\sigma}\frac{g}{c}\zeta_0 \frac{\sigma^2}{\sigma^2 - \lambda^2}\cos(\sigma t - \mu x)\,, \end{aligned} \tag{4}$$

and of (3)

$$\zeta = \frac{gh}{c^2}\frac{\sigma^2}{\sigma^2 - \lambda^2}\zeta_0 \sin(\sigma t - \mu x)$$

If the last equation is identified with (1) the velocity of progress is found:

$$c = \sqrt{gh}\sqrt{\frac{\sigma^2}{\sigma^2 - \lambda^2}} = \sqrt{gh}\sqrt{\frac{1}{1 - s^2}}, \tag{5}$$

where

$$s = \frac{\lambda}{\sigma} \tag{6}$$

Introducing this value of c in equations (4) these can be written:

$$\begin{aligned} u &= \sqrt{\frac{g}{h}}\sqrt{\frac{1}{1 - s^2}}\zeta_0 \sin(\sigma t - \mu x) \\ v &= \sqrt{\frac{g}{h}}\sqrt{\frac{s^2}{1 - s^2}}\zeta_0 \cos(\sigma t - \mu x) \end{aligned} \tag{7}$$

According to (5) the velocity of progress now depends not only upon the depth, h, but also, supposing λ to be given, upon the frequence of the wave, σ, increasing, when the frequence decreases or the period length increases. When, however, σ becomes smaller than λ, the velocity of progress becomes imaginary. This means, that waves of the kind here considered cannot exist on a rotating disc, if the frequence of the wave is smaller than the double angular velocity with which the disc rotates.

The wave motion which is characterized by equations (1) and (7) deviates essentially from the waves previously treated. In them the motion of the fluid particles alternated in or against the direction of progress, but equation (7) define a rotary motion. To the motion in the direction of progress which may be called the longitudinal is now added a motion along the wavefront which may be called transversal, and there is a phase difference of $\frac{1}{4}$ periodlength between the longitudinal and the transversal motion. If the velocities of the fluid particles are represented by a central vectordiagram, the end points of the vectors lie on an ellipse. We shall express this by saying, that the *configuration of the motion* is an *ellipse*. The ratio between the axes of the ellipse, i. e. the ratio between the min. and max. velocity, is

$$s = \frac{\lambda}{\sigma}$$

and the major axis, i. e. the max. velocity, coincides with the direction of progress and is reached when the wave reaches its max. height. The scalar value of the max. velocity is now great compared with the amplitude of the wave and the depth. viz.:

$$u_{max} = \sqrt{\frac{g}{h}} \sqrt{\frac{1}{1-s^2}} \zeta_0 , \tag{8}$$

approaching infinite values, when σ approaches λ, if ζ_0 remains finite. The direction in which the velocities rotate is negative or clockwise, if the rotation of the disc is positiv, and vice versa.

The velocity with which the wave proceeds is finally great compared with the velocity of a wave of the same period length on a resting disc.

The mean energy during one period of a column of fluid with transversal section equal to the square unit can be computed in the same way as previously (Chapter 3). We find:

$$\bar{E}_p = \frac{1}{T} g\varrho \int_0^{\zeta} \int_0^{T} z \, dz \, dt = \frac{1}{4} g\varrho \, \zeta_0^2 , \tag{9}$$

and

$$\bar{E}_k = \frac{1}{T} \varrho \int_0^{h} \int_0^{T} \frac{1}{2} (u^2 + v^2) \, dz \, dt = \frac{1}{4} g\varrho \frac{1+s^2}{1-s^2} \zeta_0^2 \tag{10}$$

and the total energy:

$$\bar{E} = \frac{1}{2} g\varrho \, \zeta_0^2 \frac{1}{1-s^2} . \tag{11}$$

According to equations (9) and (10) the potential energy is no longer equal to the kinetic, but the major part of the energy is present as kinetic.

It is of interest to determine the amplitude of the wave on the rotating disc such, that the mean energy of this wave is the same as the mean energy of a corresponding wave on a resting disc. According to equation (11) and to equation (17) of Chapter 3 we then have:

$$\frac{1}{2} g\varrho \frac{1}{1-s^2} \zeta_0^2 = \frac{1}{2} g\varrho \, \zeta'^2_0 \tag{12}$$

denoting the amplitude on the resting disc with ζ'. Of (12) we find:

$$\zeta_0 = \zeta_0' \sqrt{\frac{1}{1-s^2}} . \tag{13}$$

If the mean energy is to remain constant the amplitude must decrease with increasing velocity of rotation until the wave degenerates, when $\lambda = \sigma$.

Introducing the value of ζ_0 in the equations for the horizontal motion we find:

$$\begin{aligned} u &= \sqrt{\frac{g}{h}} \zeta_0' \sin(\sigma t - \mu x) \\ v &= s \sqrt{\frac{g}{h}} \zeta_0' \cos(\sigma t - \mu x) , \end{aligned} \tag{14}$$

where it must be remembered that ζ_0' means the amplitude of a wave with the same mean energy for $\lambda = 0$.

Comparing equations (14) with the equation for the horizontal motion in a wave of the same period length on a resting plane ((14) Chapter 3) it is found, that the longitudinal velocities remain unchanged when λ increases from zero to any value smaller than σ, but as soon as λ is different from zero transversal velocities are developed. Simultaneously the velocity of progress increases and the amplitude decreases.

The following considerations may illustrate the physical meaning of the results which are derived in this and the preceding chapter. The equations for the horizontal motion on a rotating disc differ from the corresponding equations on a resting disc by the terms:

$$-\lambda v \quad \text{and} \quad +\lambda u$$

These terms represent the force of inertia, which is generally known as the *Coriolis* force or if geophysical problems are dealt with as the deflecting force of the earth's rotation. This force is directed perpendicularly to the direction of the motion. If all other forces acting upon a body that was moving with a horizontal velocity v referred to the rotating coordinate system, suddenly ceased to act, the body would under the influence of this force of inertia continue in an orbit which in the rotating coordinat system would be a circle with radius:

$$R = \frac{v}{\lambda}.$$

The time required for one complete revolution in the inertia circle would be

$$\vartheta = \frac{2\pi}{\lambda}.$$

From the last equation we find:

$$\frac{2\pi}{\vartheta} = \lambda$$

i. e. that the frequence of the inertia-oscillation is equal to the double angular velocity of the coordinate system. If the rotation is positive the direction of revolution in the inertia circle is negative and vice versa.

The forces of inertia tend generally to preserve the kinetic energy. On an unlimited disc this tendency is not prevented by any rigid boundaries for which reason the major part of the energy in a progressive wave on a rotating disc remains kinetic. Since the force of inertia is directed perpendicularly to the velocity the transversal velocities are developed, and the particles of fluid describe ellipses. The smaller the difference between the frequence of the wave and the frequence of the inertia-oscillation, the greater is the part of the energy which remains kinetic, and the more the orbits of the fluid particles approach circles. We here meet a kind of resonance phenomenon.

In a narrow channel the vertical walls must prevent a preservation of the kinetic energy by the development of transversal motion. The force of inertia must here be balanced by a transversal slope of the wave crest, resulting in a decrease of the amplitude from one sich of the channel to the other. This may be expressed by saying, that the effect of the inertia forces is to press the wave towards one side of the channel.

7. Formal solution.

In a very wide, rotating channel a wave might perhaps be expected to be characterized by a rotary motion of the fluid particles in the middle of the channel and alterning along the walls. A wave of this kind, however, could not exist in an infinitely long channel, because the velocity of progress would vary with the distance from the walls according to the development of the rotary motion, but it seems possible, that such a wave could exist on a short stretch. A solution of the fundamental equations which satisfies the boundary conditions in this case, seems impossible, but a formal solution, which does not agree with any fixed boundary conditions may nevertheless be of value in future applications, because it represents a wave of an intermediate character compared with the waves treated in the two preceding chapters.

The equations:

$$\begin{aligned} \frac{\partial u}{\partial t} - \lambda v &= -g\frac{\partial \zeta}{\partial x} \\ \frac{\partial v}{\partial t} + \lambda u &= -g\frac{\partial \zeta}{\partial y} \end{aligned} \tag{1}$$

are satisfied by:

$$\zeta = \zeta_0 e^{-\frac{\varkappa}{c}y} \sin(\sigma t - \mu x) \tag{2}$$

$$\begin{aligned} u &= \frac{g}{c}\frac{\sigma}{\sigma - \lambda r}\zeta_0 e^{-\frac{\varkappa}{c}y} \sin(\sigma t - \mu x) \\ v &= r \cdot \frac{g}{c}\frac{\sigma}{\sigma - \lambda r}\zeta_0 e^{-\frac{\varkappa}{c}y} \cos(\sigma t - \mu x) \end{aligned} \tag{3}$$

where

$$r = \sigma\frac{\lambda - \varkappa}{\sigma^2 - \lambda\varkappa}. \tag{4}$$

and $\varkappa$ a constant. Of the equation of continuity the velocity of progress is found,

$$c = \sqrt{gh}\sqrt{\frac{1 - r^2}{(1 - sr)^2}} \tag{5}$$

where as previously $s = \frac{\lambda}{\sigma}$.

Introducing the value in (3) we find:

$$\begin{aligned} u &= \sqrt{\frac{g}{h}}\sqrt{\frac{1}{1 - r^2}}\zeta_0 e^{-\frac{\varkappa}{c}y} \sin(\sigma t - \mu x) \\ v &= \sqrt{\frac{g}{h}}\sqrt{\frac{r^2}{1 - r^2}}\zeta_0 e^{-\frac{\varkappa}{c}y} \cos(\sigma t - \mu x) \end{aligned} \tag{6}$$

These equations have the same form as equations (7) Chapter 6 except that s in replaced by r. According to equation (6) the configuration of the motion is an ellipse with the ratio r between the axises. If particularly $\varkappa = \lambda$, we find according to equation (4) and (5):

$$r = 0 \quad \text{and} \quad c = \sqrt{gh}$$

and the conditions correspond to a wave in a narrow channel; if on the other hand $\varkappa = 0$, we find:

$$r = \frac{\lambda}{\sigma} = s \quad \text{and} \quad c = \sqrt{gh}\sqrt{\frac{1}{1-s^2}}$$

i. e. we find the conditions prevailing on an unlimited disc. If generally

$$0 > \varkappa > \lambda$$

the wave is of an intermediate character; the motion is rotary, but the ratio between min. and max. velocity is smaller than on an unlimited disc. The amplitude decreases along the wave front but less rapidly than in a channel, and the velocity of progress is greater than in a channel but smaller than on an unlimited disc. The forces of inertia in this case partly preserve the kinetic energy, and are partly balanced by a transversal slope of the wavecrest.

It may be of interest to draw attention to the fact that the wave according to eq. (5) degenerates, when $r = \pm 1$. Negative values of r, supposing λ to be positive, mean that the velocities of the fluid particles rotate counter clockwise. Furthermore, the slope of the wave crest is reversed both when r is negative and when r is greater than s. It is difficult to understand that such conditions can be developed, and we shall not find any applications to these cases later on.

The other results in these chapters, however, appear to be of importance for the understanding of the tidal phenomena on the continental shelves, but before turning to the applications we shall have to study the influence of resistance on the velocities of the fluid particles, the velocity of progress and the amplitude of the wave.

III. The influence of the eddy viscosity on long, gravitational waves.

8. Viscosity and eddy viscosity.

The equations for the velocities in a long, free wave, proceeding in the direction of the positive x-axis in a viscous fluid on a resting disc, has the form:

$$\frac{\partial u}{\partial t} = \nu \frac{\partial^2 u}{\partial z^2} - g \frac{\partial \zeta}{\partial x} \tag{1}$$

where ν is the coefficient of viscosity([1]). To this equation the equation of continuity has to be added:

$$\frac{\partial \zeta}{\partial t} = -\int_0^h \frac{\partial u}{\partial x} dz \tag{2}$$

The corresponding equations for a long wave, proceeding in a fluid of uniform depth on a disc which rotates with an angular velocity $\omega = \lambda/2$, are:

$$\begin{aligned} \frac{\partial u}{\partial t} &= \lambda v + \nu \frac{\partial^2 u}{\partial z^2} - g \frac{\partial \zeta}{\partial x} \\ \frac{\partial v}{\partial t} &= -\lambda u + \nu \frac{\partial^2 v}{\partial z^2} - g \frac{\partial \zeta}{\partial y} \end{aligned} \tag{3}$$

and

$$\frac{\partial \zeta}{\partial t} = -\int_0^h \left(\frac{\partial u}{\partial x} + \frac{\partial v}{\partial y} \right) dz \tag{4}$$

A study of the influence of viscosity on long, free waves in a fluid on a resting or rotating disc, has to be based on these equations.

Lamb has shown, that the direct influence of the viscosity on tidal waves is extremely small. He considers a case in which a horizontal force

$$X = f \cos(\sigma t + \varepsilon) \tag{5}$$

is assumed to act uniformly on an unlimited layer of water of constant depth h on a resting disc. The equation for the horizontal velocities is then:

$$\frac{\partial u}{\partial t} = \nu \frac{\partial^2 u}{\partial z^2} + X \tag{6}$$

and the boundary conditions are

$$(1) \qquad u = 0 \text{ when } z = 0 \text{ and } \qquad (2) \ \frac{\partial u}{\partial z} = 0 \text{ when } z = h$$

The first condition expresses that there is no slipping motion along the bottom, the second that no tangential forces are acting on the free surface. Writing (5) in the form:

$$X = f e^{i(\sigma t + \varepsilon)} \tag{7}$$

we obtain

([1]) Lamb l. c. 542.

$$u = -\frac{if}{\sigma}\left\{1 - \frac{\cosh(1+i)\beta(h-z)}{\cosh(1+i)\beta h}\right\} e^{i(\sigma t+\varepsilon)} \tag{8}$$

where

$$\beta = \sqrt{\frac{\sigma}{2\nu}} \tag{9}$$

When βh is a large quantity, equation (8) is reduced to:

$$u = -\frac{if}{\sigma}(1 - e^{-(1+i)\beta z})\, e^{i(\sigma t+\varepsilon)}$$

or, when the imaginary part is omitted:

$$u = \frac{f}{\sigma}\left\{\sin(\sigma t+\varepsilon) - e^{-\beta z}\sin(\sigma t - \beta z + \varepsilon)\right\} \tag{10}$$

In equation (9)

$$\nu = 0.0178 \text{ gr. cm.}^{-1} \text{ sec.}^{-1},$$

the value determined for water by experiment, and

$$\frac{2\pi}{\sigma} = 12 \text{ hours}$$

are introduced, giving $\beta^{-1} = 15.6$. The last term in equation (10) disappears practically, when $\beta z = 2$, which with the numerical value for β computed above, gives $z = 31.2$ cm. This shows how imperceptible the direct influence of viscosity is upon the tidal wave. Lamb adds, however, that it cannot be doubted, that the dissipation of energy through «tidal friction», which may take place, is caused by the irregular eddies, which are formed when the velocity of the tidal currents increases in shallow water.

A motion, which is characterized by the presence of irregular eddies, is generally called turbulent. When the motion of a fluid is turbulent, it then may be conceived that every particle is moving with a certain *average* velocity to which the irregular velocities which characterize the state of turbulence are added. As a measure for the turbulence the mass of fluid which pr. square and time unit is exchanged between two neighbouring units of volume may be introduced. This quantity has been called by W. Schmidt of Vienna «die Austauschgrösse» and by L. F. Richardson the «eddy viscosity»([1]). The eddy viscosity has the same dimensions as the coefficient of viscosity and is of the greatest importance, when only the *average* velocities mentioned above are to be considered, for it can be shown, that the dynamical equations for the average velocities of a fluid in turbulent motion are formally identical with the equations for the instantaneous velocities, but that the coefficient of viscosity which enters in the last case has to be replaced by the eddy viscosity in order to make the equations valid for the average velocities.

If the laws of hydrodynamics are to be applied to problems concerning the motion of the atmosphere or the hydrosphere, we pratically always encounter the case, that only the *average* velocities are observed; the instantaneous velocities in the numerous eddies being unknown and of little or no interest. In all such cases the coefficient of viscosity must be replaced by the eddy viscosity in order to obtain agreement between observed and theoretical conditions. This was done by W. Ekman, when developing the ideas of F. Nansen, he advanced his theory of the drift-currents.

Ekman named the quantity which has here been called the eddy viscosity the *coefficient of virtual viscosity.* This coefficient in the oceanic drift currents is according to him and later investigators 1000 to 100 000 times greater than the coefficient of viscosity

[1]) Weather prediction by numerical process. Cambridge 1922, where compilation of literature.

for water. This shows, that the average velocities of the drift currents are very much affected by the enormous value of the eddy viscosity.

There is no reason why the tidal currents should be less turbulent than the drift currents. It seems judging from the results of the investigations of the drift-currents, that a study of the influence of the eddy-viscosity on the tidal phenomena can be undertaken by means of the ordinary hydrodynamical equation replacing ν with the eddy viscosity which we shall denote η. In order to see how great influence may be expected we may introduce:

$$\eta = 10\,000\,\nu = 178 \text{ gr. cm.}^{-1} \text{ sec.}^{-1}$$

in equation (9) and obtain then, making as previously $\frac{2\pi}{\sigma} = 12$ hours, $\beta^{-1} = 1560$. From this result it is evident that the last term in equation (10) is perceptible even at a distance of $z = 3000$ cm. $= 30$ m. from the bottom. It may, therefore, be expected that the velocities of the tidal currents and furthermore the height and the rate of progress of the tidal wave in shallow water are modified on account of the resistance arising from the irregular eddies.

A study of these modifications may be based on the equations (1) to (4) or if restricted to the conditions on a resting plane on the equations (5) and (6) used by Lamb combined with the equation of continuity. The latter are, however, less adapted for the purpose because the the height and length of the wave do not appear explicitly. We shall for this reason make use of the first named only. The intention is, as emphasized, to investigate the influence of the eddy viscosity on the average velocities and on the height and wave length but since the equations are formally identical with the dynamical equations for a viscous fluid, all results can be applied to long waves in a viscous fluid by absence of turbulence by replacing the eddy viscosity with the ordinary viscosity.

It may be of advantage before proceeding further to discuss the eddy-viscosity briefly. The main difficulty that we shall meet, is that the eddy viscosity is far from being constant. The variations of the eddy viscosity in the sea have not been much studied but the corresponding variations of the eddy viscosity in the air have been made subject to extensive investigations. The conditions in the sea and the air are closely related, for which reason it is justifiable to assume that the rules for the variation of the eddy viscosity in the air are valid for the corresponding variations in the sea. On the ground itself the turbulence must be zero and observations show, that the eddy viscosity directly above the ground is very small. The eddy viscosity increases very rapidly when ascending from the ground, and even from a distance of about 10 meters and upwards attains an amount, which on an average seems to be constant but which in single cases mainly depends upon the stability of the atmosphere towards vertical displacements. The eddy viscosity is very small if the stability is great, when for instance the temperature increases with altitude, because the stability then is a direct hindrance against the exchange of air between different horizontal layers. On the other hand, the eddy viscosity is very large in unstable equilibrium.

An introduction of an eddy-viscosity which varies with altitude gives the equations which are to be integrated, a form which cannot be solved unless very special assumptions regarding the variation with altitude are made. This introduction, therefore, is of small value, but by assuming a constant eddy viscosity valuable results have been derived, e. g. regarding the variation of the wind with altitude. If it is supposed, that no slipping motion exists along the ground, a qualitative agreement between the theoretical and the observed change of the wind is found, but the quantitative agreement is poor, particularly because the velocity of the wind increases far more in the lowest meters

above the ground than required by the theory. This is evidently caused by the rapid increase in the eddy viscosity directly above the ground. It is possible to obtain a better agreement, except for the lowest layer by introducing an emperical law for the resistance against the motion of the layer immediately above the ground and, as previously, regard the eddy viscosity as constant above this layer. The main point is, however, in this connection that valuable results are obtained when the eddy viscosity is regarded as constant in spite of the great variations which this quantity may show in single cases.

Applying these results to the present problem, we may expect to obtain results which give qualitative agreement with the observed values by assuming no slipping motion along the bottom, and a constant eddy-viscosity from the bottom and upward, but it is not unlikely, that better quantitative agreement can be obtained by assuming that a layer close to the bottom glides along the latter. We shall try to solve the equations in both cases. Furthermore we shall consider a wave, which is propagating between two boundaries, the lower rigid and the upper of such a nature, that it makes no resistance towards vertical, but a great resistance against horizontal diplacements. This case is of particular interest for the study of the progress of the tidal wave in a shallow, ice-covered sea like that on the North Siberian shelf.

9. General solution for waves in an unlimited layer.

The general equations on page 26 have been solved only for waves proceeding on an unlimited disc in a layer of homogeneous fluid of constant depth. We shall, therefore, at once turn to this case. We shall as previously (Chapter 6) assume, that the wave varies in the direction perpendicular to the wave front only. This direction will be chosen as x-axis. The equation (3) and (4), Chapter 8, in which we have now to replace ν by η, then take the form:

$$\begin{aligned} \frac{\partial u}{\partial t} - \lambda v - \eta \frac{\partial^2 u}{\partial z^2} &= -g \frac{\partial \zeta}{\partial x} \\ \frac{\partial v}{\partial t} + \lambda u - \eta \frac{\partial^2 v}{\partial z^2} &= 0 \end{aligned} \tag{1}$$

and

$$\frac{\partial \zeta}{\partial t} = -\int_0^h \frac{\partial u}{\partial x}\, dz \tag{2}$$

In these equations u and v designate average velocities as defined above. It is evident that only these average velocities enter in the equation of continuity, because the convergences or divergences in the numerous eddies are of no account for the height of the wave.

We have previously seen that equations (1) and (2), omitting the terms representing the influence of the eddy viscosity, are satisfied by

$$\zeta = \zeta_0 \sin(\sigma t - \mu x) \tag{3}$$

According to this equation the maximum height of the wave is independent of x. This involves, as we have seen, the circumstances that the energy of the wave is constant and independent of x. This solution can no longer be valid, because the energy of the wave is dissipated through the turbulent motions and consequently the energy and the height of the wave must decrease in the direction in which the wave proceeds. As an assumption we shall therefore introduce:

$$\zeta = f(x) \sin(\sigma t - \mu x), \tag{4}$$

where $f(x)$ represents an unknown function. Writing:

$$\zeta = -if(x)\, e^{i(\sigma t - \mu x)} \tag{5}$$

we obtain

$$\frac{\partial u}{\partial t} - \lambda v - \eta \frac{\partial^2 u}{\partial z^2} = g\left\{\mu f(x) + i f'(x)\right\} e^{i(\sigma t - \mu x)} \tag{6}$$

$$\frac{\partial v}{\partial t} + \lambda u - \eta \frac{\partial^2 v}{\partial z^2} = 0$$

Eliminating v we obtain an equation with u only that is satisfied by the value:

$$u = \frac{1}{\sigma^2 - \lambda^2} g\left\{i\mu f(x) - f'(x)\right\}\left\{C_1 e^{(1+i)\beta_1 z} + C_2 e^{-(1+i)\beta_1 z} + C_3 e^{(1+i)\beta_2 z} + C_4 e^{-(1+i)\beta_2 z} - \sigma\right\} e^{i(\sigma t - \mu x)} \tag{7}$$

where C_1, C_2, C_3 and C_4 are constants which are to be determined by the boundary conditions and where:

$$\beta_1 = \sqrt{\frac{\sigma + \lambda}{2\eta}} \quad \beta_2 = \sqrt{\frac{\sigma - \lambda}{2\eta}} \tag{8}$$

The function $f(x)$ can now be determined by means of the equation of continuity which leads to

$$-g \frac{1}{\sigma^2 - \lambda^2}\left\{\mu^2 f(x) + i\,2\mu f'(x) - f''(x)\right\} \int_0^h \varphi(z)\, dz = \sigma\, (f(x) \tag{9}$$

where $\varphi(z)$ represents the term in the last brackets in equation (7).

Equation (9) is evidently satisfied by

$$f(x) = \zeta_0 e^{-\gamma x} \tag{10}$$

provided that μ and γ are roots in the equation:

$$-g \frac{1}{\sigma^2 - \lambda^2}\left\{\mu^2 - i\,2\mu\gamma - \gamma^2\right\} \int_0^h \varphi(z)\, dz = \sigma \tag{11}$$

The exponent γ will be called the exponent of damping. We thus arrive to the result, that the amplitude of the wave changes in the direction of progress according to the exponential law expressed by (10).

Of equation (11) we shall not seek the quantities μ and γ, but instead the velocity with which the wave proceeds:

$$c = \frac{L}{T} = \frac{\sigma}{\mu} \tag{12}$$

and the ratio p, which later will be referred to as the coefficient of damping,

$$p = \frac{\gamma}{\mu} \tag{13}$$

Equation (11) can then be written.

$$\frac{\sigma}{\sigma^2 - \lambda^2} \frac{g}{c^2} (p + i)^2 \int_0^h \varphi(z)\, dz = 1. \tag{14}$$

Introducing the value of $f(x)$ in the equation for u, and computing v by means of (6), we finally get:

$$u = \frac{\sigma}{\sigma^2 - \lambda^2}\frac{g}{c}\zeta_0 e^{-\gamma z}(p+i)\left[C_1 e^{(1+i)\beta_1 z} + C_2 e^{-(1+i)\beta_1 z} + C_3 e^{(1+i)\beta_2 z} + C_4 e^{-(1+i)\beta_2 z} - \sigma\right] e^{i(\sigma t - \mu x)}$$
$$v = \frac{\sigma}{\sigma^2 - \lambda^2}\frac{g}{c}\zeta_0 e^{-\gamma z}(p+i)\left[-C_1 e^{(1+i)\beta_1 z} - C_2 e^{-(1+i)\beta_1 z} + C_3 e^{(1+i)\beta_2 z} + C_4 e^{-(1+i)\beta_2 z} - \lambda\right] e^{i(\sigma t - \mu x)} \quad (15)$$

These equations are valid for all values of σ, which are greater than λ. If the original wave is composed of several waves

$$\zeta = -\Sigma i \zeta_{o,n} e^{i(\sigma_n t - \mu_n x)}$$

where $\sigma_n > \lambda$ the velocities can be represented by a corresponding number of equations of the same form as (15).

The equations (14) and (15) will now be further discussed by determining the constants C_1 to C_4 by means of varying boundary conditions.

10. Free surface and no slipping motion along the bottom.

We will at first suppose that no slipping motions take place along the bottom. The boundary conditions are then

$$z = 0,\ u = v = 0$$
$$\text{and}\quad z = h,\ \frac{\partial u}{\partial z} = \frac{\partial v}{\partial z} = 0$$

where the last condition again means that no tangential forces are acting upon the free surface. Determining the constants C_1 to C_4 by means of these conditions we obtain:

$$u = -\frac{\sigma^2}{\sigma^2 - \lambda^2} g \frac{\zeta_0}{c} e^{-\gamma z}(p+i)\left[1 - \frac{1}{2}\frac{\sigma - \lambda}{\sigma}\frac{\cosh(1+i)\beta_1(h-z)}{\cosh(1+i)\beta_1 h} - \right.$$
$$\left. - \frac{1}{2}\frac{\sigma - \lambda}{\sigma}\frac{\cosh(1+i)\beta_2(h-z)}{\cosh(1+i)\beta_2 h}\right] e^{i(\sigma t - \mu x)}$$
$$v = -i\frac{\sigma^2}{\sigma^2 - \lambda^2} g \frac{\zeta_0}{c} e^{-\gamma z}(p+i)\left[\frac{\lambda}{\sigma} + \frac{1}{2}\frac{\sigma - \lambda}{\sigma}\frac{\cosh(1+i)\beta_1(h-z)}{\cosh(1+i)\beta_1 h} \right. \quad (1)$$
$$\left. - \frac{1}{2}\frac{\sigma + \lambda}{\sigma}\frac{\cosh(1+i)\beta_2(h-z)}{\cosh(1+i)\beta_2 h}\right] e^{i(\sigma t - \mu x)}$$

and:

$$-\frac{gh}{c^2}\frac{\sigma^2}{\sigma^2 - \lambda^2}(p+i)^2\left[1 - \frac{1}{2}\frac{\sigma - \lambda}{\sigma}\frac{1-i}{2\beta_1 h}\operatorname{tgh}(1+i)\beta_1 h \right.$$
$$\left. - \frac{1}{2}\frac{\sigma + \lambda}{\sigma}\frac{1-i}{2\beta_2 h}\operatorname{tgh}(1+i)\beta_2 h\right] = 1. \quad (2)$$

Omitting the imaginary parts of (1) we get:

$$u = \frac{\sigma^2}{\sigma^2 - \lambda^2}\frac{g\zeta_0}{c} e^{-\gamma z}\left[(1 - qa_1 - ra_2 + pq\,b_1 + prb_2)\sin(\sigma t - \mu x) - \right.$$
$$\left. - p\left(1 - qa_1 - ra_2 - \frac{q}{p}b_1 - \frac{r}{p}b_2\right)\cos(\sigma t - \mu x)\right]$$
$$v = \frac{\sigma^2}{\sigma^2 - \lambda^2}\frac{g\zeta_0}{c} e^{-\gamma z}\left[\left(\frac{\lambda}{\sigma} + qa_1 - ra_2 - pq\,b_1 + prb_2\right)\cos(\sigma t - \mu x) + \right. \quad (3)$$
$$\left. + p\left(\frac{\lambda}{\sigma} + qa_1 - ra_2 + \frac{q}{p}b_1 - \frac{r}{p}b_2\right)\sin(\sigma t - \mu x)\right]$$

where:

$$q = \frac{1}{2}\frac{\sigma - \lambda}{\sigma}, \quad r = \frac{1}{2}\frac{\sigma + \lambda}{\sigma} \tag{4}$$

$$a_1 = \frac{\cosh \beta_1 (2h - z) \cos \beta_1 z + \cosh \beta_1 z \cos \beta_1 (2h - z)}{\cosh 2\beta_1 h + \cos 2\beta_1 h} \tag{5}$$

and

$$b_1 = \frac{\sinh \beta_1 (2h - z) \sin \beta_1 z + \sinh \beta_1 z \sin \beta_1 (2h - z)}{\cosh 2\beta_1 h + \cos 2\beta_1 h} \tag{6}$$

and where the expressions for a_2 and b_2 are similar those for a_1 and b_1 except that β_1 is replaced by β_2. Separating the real and imaginary parts of (2) we find:

$$2p(1 - qA_1 - rA_2) + (p^2 - 1)(qB_1 + rB_2) = 0 \tag{7}$$

and

$$\frac{\sigma^2}{\sigma^2 - \lambda^2}\frac{gh}{c^2}\left[(1 - p^2)(1 - qA_1 - rA_2) + 2p(qB_1 + rB_2)\right] = 1 \tag{8}$$

where:

$$A_2 = \frac{1}{h}\int_0^h a_1 \, dz = \frac{1}{2\beta_1 h}\frac{\sinh 2\beta_1 h + \sin 2\beta_1 h}{\cosh 2\beta_1 h + \cos 2\beta_1 h}$$

$$B_1 = \frac{1}{h}\int_0^h b_1 \, dz = \frac{1}{2\beta_1 h}\frac{\sinh 2\beta_1 h - \sin 2\beta_1 h}{\cosh 2\beta_1 h + \cos 2\beta_1 h}$$

and where A_2 and B_2 are expressed similarly to A_1 and B_1, replacing β_1 by β_2.

We shall at first discuss equations (7) and (8). These are not well adapted for an analytical discussion, and it is therefore necessary to compute numerical values of p and c for various values of βh and $\frac{\lambda}{\sigma}$. The coefficients A_1 B_1 A_2 and B_2 can in fact be regarded as functions of βh and s because according to (8) Chapter 9 and (9) Chapter 8 we have

$$\beta_1 = \sqrt{\frac{\sigma + \lambda}{2\eta}} = \sqrt{1 + s}\,\beta \text{ and } \beta_2 = \sqrt{\frac{\sigma - \lambda}{2\eta}} = \sqrt{1 - s}\,\beta \tag{11}$$

where

$$s = \frac{\lambda}{\sigma}. \tag{12}$$

The coefficients q and r are functions of s only.

Instead of tabulating c we shall tabulate the ratio

$$\frac{c}{c_0} = w \tag{13}$$

where

$$c_0 = \sqrt{gh}\sqrt{\frac{\sigma^2}{\sigma^2 - \lambda^2}} \tag{14}$$

the velocity which the wave should have by absence of turbulence.

The result of the numerical computations is given in Tables 6 and 7. From these Tables new values have to be derived in order to be interpreted, because we are not concerned with the quantitatives p and w but have to discuss how the exponent of damping γ, and the actual velocity of progress c, vary under different conditions. Before

doing this it may be of advantage to repeat the relations between these different quantities. According to (13) and (14) we have

$$c = w(\beta h, s)\sqrt{gh}\sqrt{\frac{1}{1-s^2}} \tag{15}$$

where by writing $w(\beta h, s)$ we indicate that w is a function of βh and s.

Table 6.

The ratio $p = \frac{\gamma}{\mu}$ as function of βh and s.

βh	$s = \frac{\lambda}{\sigma}$			
	0.0	0.3	0.6	0.9
0.2	0.97	0.97	0.98	0.98
0.4	0.88	0.88	0.89	0.90
0.6	0.75	0.76	0.77	0.78
0.8	0.61	0.63	0.65	0.69
1.0	0.48	0.51	0.57	0.68
1.2	0.38	0.40	0.50	0.67
1.4	0.30	0.33	0.44	0.67
1.6	0.24	0.27	0.39	0.67
1.8	0.20	0.23	0.34	0.66
2.0	0.16	0.19	0.29	0.63
2.5	0.124	0.140	0.212	0.57
3.0	0.099	0.105	0.162	0.48
4.0	0.071	0.080	0.100	0.34
5.0	0.055	0.061	0.084	0.23
∞	0.000	0.000	0.000	0.000

Table 7.

The ratio $\frac{c}{c_0}$ as function of βh and s.

βh	$s = \frac{\lambda}{\sigma}$			
	0.0	0.3	0.6	0.9
0.2	0.22	0.22	0.19	0.09
0.4	0.43	0.41	0.36	0.18
0.6	0.60	0.57	0.48	0.26
0.8	0.72	0.70	0.58	0.30
1.0	0.79	0.77	0.65	0.35
1.2	0.84	0.82	0.71	0.40
1.4	0.86	0.84	0.76	0.46
1.6	0.88	0.87	0.80	0.51
1.8	0.89	0.88	0.84	0.56
2.0	0.90	0.89	0.86	0.61
2.5	0.92	0.91	0.88	0.72
3.0	0.93	0.92	0.90	0.78
4.0	0.94	0.93	0.92	0.84
5.0	0.95	0.95	0.93	0.88
∞	1.00	1.00	1.00	1.00

Correspondingly, we write.

$$\gamma = p(\beta h, s)\,\mu \tag{16}$$

Introducing

$$\mu = \frac{2\pi}{c\,T} \tag{17}$$

where T means the period length of the wave, we obtain from (16) and (15):

$$\gamma = \frac{1}{T}\cdot\frac{2\pi}{\sqrt{gh}}\sqrt{1-s^2}\cdot\frac{p(\beta h, s)}{w(\beta h, s)} \tag{18}$$

We may now discuss the velocity of progress under various conditions. We have then to remind ourselves of the definition of β

$$\beta = \sqrt{\frac{\sigma}{2\eta}} = \sqrt{\frac{\pi}{T\eta}} \tag{19}$$

showing that βh depends not only on η and h but also on T. From this it may at once be concluded that the velocity of progress is no longer the same for waves of different periods, even on a resting disc, assuming η and h to be constant, but that it varies with

the length of the period. We shall, however, at first regard T as constant in order to find how c varies with βh and λ, For this purpose we write

$$c = \sqrt{gh} \cdot w(\beta h, s) f(s) \tag{20}$$

By means of the tabulated values of w we can derive the relative values of c that are compiled in Table 8.

Table 8.

$\frac{c}{\sqrt{gh}}$ as function of βh and s assuming T constant.

βh	s			
	0.0	0.3	0.6	0 9
0.5	0.52	0.52	0.52	0.50
1.0	0.79	0.81	0.81	0.81
2.0	0.90	0.93	1.06	1.41
3.0	0.93	0.96	1.12	1.78
4.0	0.94	0.98	1.15	1.92
5.0	0.95	0.99	1.16	2.01
∞	1.00	1.05	1.25	2.29

The first striking feature is that the velocity of progress by presence of eddy-viscosity is always *smaller* than the corresponding velocity for $\eta = 0$ ($\beta h = \infty$), the next, that the reduction of the velocity is much greater on a rotating than on a resting disc. This leads us to the circumstance that the velocity for very small values of βh decreases in increasing speed of rotation, but for greater values of βh the normal increase is found though smaller than in absence of turbulence. Small values of βh correspond by given values of h to great values of η and vice versa.

We will next turn to the velocity of progress for waves of various period lengths. The conditions, however, are essentially different on a rotating and a resting disc for which reason it is necessary to treat the two cases separately.

We will first regard the conditions on a resting plane ($s = 0$) where

$$c = \sqrt{gh}\, w(\beta h) \tag{21}$$

We may select a wave of a given period length T_1 and compare the velocity of this wave with the corresponding velocities of waves of the period lengths $T = n T_1$ where n may have any value between 0 and ∞.

For this purpose we write

$$\beta = \sqrt{\frac{2\pi}{n T_1 \eta}} = \frac{1}{\sqrt{n}} \cdot \beta_1 \tag{22}$$

where β_1 evidently means the value of β corresponding to the assumed values of T_1 and η. Introducing 22) in (21) we obtain

$$c = \sqrt{gh}\; w\left(\frac{1}{\sqrt{n}, \beta_1 h}\right) \tag{23}$$

and can tabulate c as a function of n for various values of $\beta_1 h$. The result is compiled in Table 9.

Table 9.

$\frac{c}{\sqrt{gh}}$ for waves of various relative period lengths on a resting disc.

$\beta_1 h$	n			
	1	2	3	4
0.5	0.52	0.38	0.32	0.28
1.0	0.79	0.68	0.59	0.52
2.0	0.90	0.87	0.83	0.79
3.0	0.93	0.91	0.89	0.87
4.0	0.94	0.92	0.91	0.90
5.0	0.95	0.94	0.92	0.92
∞	1.00	1.00	1.00	1.00

We are only here concerned with the variation withen the rows because the variations within the columns which depend upon variations of $\beta_1 h$ by constant value of T have already been discussed. The table shows that the velocity in given values of η and h decreases with the length of the period. The shorter waves travel *faster* than the longer on a resting disc.

On a rotating disc the conditions are far more complicated. We may again introduce

$$T = n\,T_1$$

and obtain

$$s = \frac{\lambda}{\sigma} = n \cdot \frac{\lambda}{\sigma_1} = n s_1 \tag{24}$$

Equation (15) may then be written:

$$c = \sqrt{gh} \cdot w(\beta_1 h, s_1, n) \sqrt{\frac{1}{1 - n^2 s_1^2}} \tag{25}$$

We may, therefore, proceed in such a manner, that we select a value of s_1 and tabulate c for various values of $\beta_1 h$ and n, but we have to consider that no values of n are allowed that make $s = n s_1 > 1$. It does not matter what value we choose for s_1. If we make s_1 small we may study all possible cases with the above mentioned restriction by giving n values larger than 1, if we choose s_1 close to 1 we may give n values smaller than 1. We may chose $s_1 = 0.3$ and give n the values 1, 2 and 3. The result of the computation is represented in Table 10.

Table 10.

$\frac{c}{\sqrt{gh}}$ for waves of various length of period on a rotating plane.

$\beta_1 h$	$n = 1$	2	3
0.5	0.52	0.40	0.31
1.0	0.81	0.67	0.57
2.0	0.93	0.96	0.90
3.0	0.96	1.08	1.25
4.0	0.98	1.11	1.57
5.0	0.99	1.14	1.76
∞	1.05	1.25	2.29

We are again concerned with the variations within the rows only. These show that the law already stated for waves on a resting disc only holds good for small values of $\beta_1 h$, only then do the shorter waves travel fastest. When βh is large the conditions are reversed, the longest waves have the greatest velocities. In intermediate values of βh a maximum of velocity is found in a certain period length, both shorter and longer waves proceed with smaller velocities.

A numerical example may illustrate the content of the tables. Assuming $T_1 = 12$ hours viz. $\sigma = \frac{2\pi}{12 \cdot 3600} = 1.45 \cdot 10^{-4}$, $h = 30$ m. $= 3.10^3$ cm. and $\eta = 163$ gr.cm.$^{-1}$sec.$^{-1}$, we find $\beta = 0.667 \cdot 10^{-3}$ and $\beta h = 2.0$. From Table 8 we learn, that this wave proceeds on a resting disc ($s = 0$) with a velocity $c = \sqrt{gh} \cdot 0.90 = 15.4$ m/sec. If the disc rotates with an angular velocity $\omega = \frac{\lambda}{2} = 0.22 \cdot 10^{-4}$ making $s = 0.3$ we find

$$c = \sqrt{gh} \cdot 0.93 = 15.9 \text{ m/sec.}$$

If ω increases to $0.435 \cdot 10^{-4}$ or $0.655 \cdot 10^{-4}$ we find the corresponding velocities to be respectively

$$c = \sqrt{gh} \cdot 1.00 = 18.2 \text{ m/sec. and } c = \sqrt{gh} \cdot 141 = 24.1 \text{ m/sec.}$$

From Table 9 we find that a wave with the double period length, $T = 24$ hours, on a resting disc proceeds with the velocity

$$c = \sqrt{gh} \cdot 0.87 = 14.9 \text{ m/sec.}$$

If the period length increases to 36 or 48 hours we find the corresponding velocities

$$c = \sqrt{gh} \cdot 0.83 = 14.2 \text{ m/sec. and } c = \sqrt{gh} \cdot 0.79 = 13.5 \text{ m/sec.}$$

From Table 10 we find that a wave with the double period length, $T = 24$ hours on a disc which rotates with an angular velocity $\omega = 0.22 \cdot 10^{-4}$ proceeds with a velocity

$$c = \sqrt{gh} \cdot 0.96 = 16.5 \text{ m/sec.}$$

and that the velocity of a wave with a period length of 36 hours is

$$c = \sqrt{gh} \cdot 0.90 = 15.4 \text{ m/sec.}$$

The relative values of the exponent of damping, γ, can be represented by a set of similar tables. The considerations which lead to the various forms of the tables are the same and a repetition of these is unnecessary.

Table 11 corresponds to Table 8 and shows the relative variations of γ with βh and s, assuming T to be constant.

Table 11.

$\gamma \cdot \frac{\sqrt{gh}}{\sigma}$ as function of βh and s, assuming T constant.

βh	s			
	0.0	0.3	0.6	0.9
0.5	1.57	1.58	1.60	1.66
1.0	0.61	0.63	0.70	0.84
2.0	0.18	0.20	0.28	0.45
3.0	0.11	0.12	0.14	0.27
4.0	0.07	0.08	0.09	0.18
5.0	0.06	0.06	0.07	0.12
∞	0.00	0.00	0.00	0.00

The damping increases by increasing velocity of rotation, and the increase is much greater in larger values of βh than in smaller. The ratio between the exponents for $s = 0.9$ and $s = 0.0$ has for $\beta h = 0.5$ the value 1.06 for $\beta h = 5.0$ the value 2.0.

Table 12 corresponds to Table 9 and shows how waves of various period lengths are damped on a resting disc.

Table 12.

$\gamma \frac{\sqrt{gh}}{\sigma}$ for waves of various period lengths on a resting disc.

$\beta_1 h$	$n = \frac{T_1}{T}$			
	1	2	3	4
0.5	1.57	1.06	0.93	0.82
1.0	0.61	0.50	0.43	0.39
2.0	0.18	0.17	0.16	0.15
3.0	0.11	0.085	0.078	0.076
4.0	0.075	0.060	0.050	0.045
5.0	0.058	0.047	0.038	0.033
∞	0.000	0.000	0.000	0.000

The main result of this table is, that the shorter waves are damped more rapidly than the longer. The difference in the damping is greatest for very small values of βh and considerable for large values, but has a marked minimum for intermediate values.

On a rotating disc the conditions are far more complicated. This is evident from Table 13, which corresponds to Table 10, and contains the relative values of γ for waves of various period lengths assuming $s = 0.3$ for the shortest wave.

Table 13.

$\gamma \frac{\sqrt{gh}}{\sigma_1}$ for waves of various period lengths on a rotating disc assuming $s_1 = 0.3$ for the shortest wave.

$\beta_1 h$	n		
	1	2	3
0.5	1.58	1.14	1.14
1.0	0.63	0.53	0.46
2.0	0.20	0.23	0.25
3.0	0.118	0.125	0.18
4.0	0.082	0.078	0.127
5.0	0.063	0.054	0.095
∞	0.000	0.000	0.000

We find for small values of $\beta_1 h$ the rule which was stated for waves on a resting plane; the shorter waves are damped more rapidly than the longer. The same rule is also valid for larger values of $\beta_1 h$, if the value of $s = n s_1$ for the waves which are regarded is considerably smaller than 1. For intermediate values of $\beta_1 h$ we find the rule reversed; the longer waves are damped most rapidly and the same is true even for greater values of $\beta_1 h$ if $s = n s_1$ approaches 1.

As a numerical example we may introduce the same values for T, h and η as previously, obtaining $\beta h = 2.0$. From Table 11 we learn that the exponent of damping for this wave on a resting disc ($s = 0$) is

$$\gamma = \frac{\sigma}{\sqrt{gh}} \cdot 0.18 = 0.15 \cdot 10^{-7} \text{ cm.}^{-1}$$

The amplitude of the wave can therefore be expressed by the equation

$$\zeta = \zeta_0 e^{-0.15 \cdot 10^{-7} x}$$

where x is measured in cms.. Expressing x in kilometers we find

$$\zeta = \zeta_0 e^{-0.15 \cdot 10^{-2} x}$$

The amplitude consequently decreases over a distance of 100 km. to

$$\zeta = 0.86 \, \zeta_0$$

and over a distance of 1000 km. to

$$\zeta = 0.23 \, \zeta_0$$

An extension of the example along the lines followed on page 36 seems unnecessary. The preceding discussion shows that the waves are greatly influenced by the eddy-viscosity and shows the lines along which these modifications take place.

We will next turn to a brief discussion of the velocities of the particles of fluid. These are still more complicated than the rate of progress and the damping of the wave because they depend on all the variables already dealt with, and furthermore upon t, x, z and ζ_0.

From equations (3) it is evident that the variations with t, x and ζ_0 are simple. The amplitudes of the velocity components are proportional to ζ and the amplitudes and the phase angles decrease, when x increases from x_1 to x_2, the first in the ratio $e^{-\gamma x_2} : e^{-\gamma x_1}$, the latter with the amount $\mu (x_2 - x_1)$ where γ and μ under the given conditions have to be determined by means of the equations (7) and (8), or the preceding tables.

The equations (3) are else not adapted to analytical discussion, for which reason it again is necessary to compute numerical values in order to demonstrate how the character of the motion varies with the distance from the boundary surface, z, under different conditions. Making $x = 0$, equations (3) can be written in the form:

$$\begin{aligned} u &= (M \cos \sigma t + N \sin \sigma t) \frac{\sigma^2}{\sigma^2 - \lambda^2} g \frac{\zeta_0}{c} \\ v &= (P \cos \sigma t + Q \sin \sigma t) \frac{\sigma^2}{\sigma^2 - \lambda^2} g \frac{\zeta_0}{c}, \end{aligned} \tag{26}$$

where the meaning of the letters M, N, P and Q is evident by comparison with (3).

These equations define the curve, which during one period is described by the end point of the vector which represents the velocity, previously called the configuration of the motion. It can easily be shown that any set of equations of the form (26) represents

an ellipse and consequently we learn from (26) that the configuration of the motion is elliptical in all depths and under all conditions. The motion in any depth can therefore be fully described by means of the following four quantities (see Fig. 5).

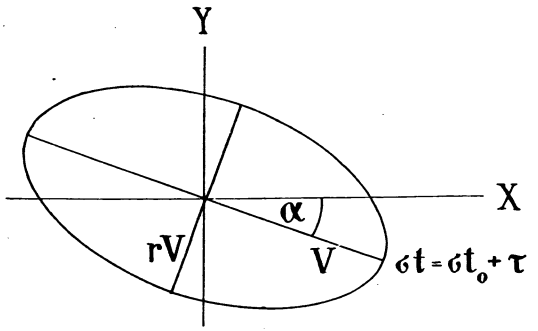

Fig. 5.

1. The scalar value of maximum velocity, V.
2. The ratio between the scalar values of minimum and maximum velocity, r.
3. The angle of orientation which the major axis of the ellipse forms with the positive x-axis, a.
4. The phase difference expressed in degrees between time of maximum velocity and time of maximum wave-height, τ.

These four quantities can be computed from the coefficients M, N, P and Q by means of the following formula, which can be derived by simple reckoning(1):

$$2V = \frac{\sigma^2}{\sigma^2 - \lambda^2} \frac{g}{c} \zeta_0 \sqrt{(M+Q)^2 + (N-P)^2} + \sqrt{(M-Q)^2 + (N+P)^2} \tag{27}$$

$$2rV = \frac{\sigma^2}{\sigma^2 - \lambda^2} \frac{g}{c} \zeta_0 \sqrt{(M+Q)^2 + (N-P)^2} - \sqrt{(M-Q)^2 + (N+P)^2} \tag{28}$$

$$\operatorname{tg} 2\alpha = \frac{MP + NQ}{(M^2 + N^2) - (P^2 + Q^2)} \tag{29}$$

$$\operatorname{tg} 2\tau = \frac{MN + PQ}{(M^2 + P^2) - (N^2 + Q^2)} \tag{30}$$

The sign of the minimum velocity, rV, indicates the direction in which the velocity rotates. In positive, or counter-clockwise rotation of the velocity, the sign is positive, in clockwise rotation, it is negative.

The sign of the angle a is positive if the maximum velocity, corresponding to maximum height of the wave, lies to the left of the x-axis, negative if it lies to the right. The maximum velocity is reached before the wave reaches maximum height if τ is negative, and after if τ is positive.

The maximum velocity itself will be expressed in fractions of the velocity which would be found on a resting plane with absence of eddy viscosity, supposing the ampli-

(1) W. Werenskiold: An analysis of current-measurements in the open sea. Det 16de skand. naturforskermøte, 1916 p. 360—383.

tude to be ζ_0. This maximum velocity which will be called normal according to (14) Chapter 3 is:

$$V_0 = \sqrt{gh} \cdot \frac{\zeta_0}{h} \tag{31}$$

Introducing (31) and (15) p. 33 in equation (27) we find:

$$\frac{V}{V_0} = \sqrt{\frac{\sigma^2}{\sigma^2 - \lambda^2}} \cdot \frac{1}{2} \cdot \frac{\sqrt{(M+Q)^2 + (N-P)^2} + \sqrt{(M-Q)^2 + (N+P)^2}}{w\,(\beta h, s)} \tag{32}$$

The square roots have to be computed by means of equation (3) and the value of w to be introduced from Table 8.

If $s = 0$ we have $v = 0$ and the ellipse is degenerated to a straight line, coinciding with the direction of the x-axis. In any depth the motion can then be characterized by the two quantities $\frac{V}{V_0}$ and τ.

Tables 14 and 15 contain the computed values of these quantities for various values of βh and βz.

Table 14.

$\frac{V}{V_0}$ as function of βh and βz; $s = 0$.

βz	βh			
	0.5	2.0	5.0	∞
0.5	0.60	0.63	0.57	0.54
1.0		1.06	0.90	0.86
2.0		1.32	1.12	1.06
5.0			1.05	1.00
∞				1.00

Table 15.

τ as function of βh and βz; $s = 0$.

βz	βh			
	0.5	2 0	5.0	∞
0.5	— 38°	— 22°	— 28°	— 28°
1.0		— 12°	— 18°	— 18°
2.0		— 3°	— 4°	— 4°
5.0			0°	0°
∞				0°

The content of these tables is perhaps best illustrated by an example. Assuming $\beta h = 5.0$ we find from Table 14 that the max. velocity at the surface, $\beta z = \beta h$, is 1.05 times greater than it would have been with absence of turbulence, and from Table 15, that it occurs when the wave reaches the maximum height. At a distance from the bottom $z = 0.1\,h$ corresponding to $\beta z = 0.5$ the maximum velocity is 0.57 of the normal and occurs 28° earlier than at the surfaces. The result that the velocities at the surface with presence of turbulence can exceed the normal values considerably, is accounted for by the fact that the gradients of the wave are increased because the velocity of progress has been reduced.

The main result which will be emphasized is, that the max. velocities decrease towards the bottom and here occur at an earlier moment than at the surface.

We shall next assume

$$\frac{\lambda}{\sigma} = s = 0.9.$$

In this case the velocities are rotary and we have to compute the ratio between the axes and the angle of orientation of the ellipse that represents the configuration of the motion in order to describe this in an exhaustive way. The four quantities which characterize the motion have been compiled in Tables 16 to 19 for various values of βh and βz. We

may again take a numerical example. Assuming $\beta h = 5.0$, we find, that the maximum velocity at the surface, $\beta z = \beta h$, is 2.92 times greater than it had been on a resting plane with absence of eddy viscosity, it is reached 2° after the wave has attained the maximum height, and is directed 12° to the right of the direction in which the wave propagates. The ratio between the minimum and maximum velocities is — 0.91, where the sign — indicates that the velocity rotates clockwise. In the distance $z = 0.1\ h$ from the boundary surface the maximum velocity is only 0.69 times the normal; it occurs 24° earlier than at the surface, is deviated slightly less from the x-axes, and the ratio between minimum and maximum velocity has decreased to — 0.69.

Table 16.

$\frac{V}{V_0}$ as function of βh and βz; $s = 0.9$.

βz	βh			
	0.5	2.0	5.0	∞
0.5	0.62	0.90	0.69	0.54
1.0		1.50	1.10	0.96
2.0		1.94	1.76	1.54
5.0			2 92	2.35
∞				2 29

Table 17.

τ as function of βh and βz; $s = 0.9$.

βz	βh			
	0.5	2 0	5.0	∞
0.5	— 37°	— 16°	— 22°	— 29°
1.0		— 10°	— 10°	— 25°
2.0		— 5°	— 3°	— 18°
5.0			2°	— 10°
∞				0°

Table 18.

r as function of βh and βz; $s = 0.9$.

βz	βh			
	0.5	2.0	5.0	∞
0.5	— 0.03	— 0.65	— 0.69	— 0.68
1.0		— 0.71	— 0.78	— 0.75
2.0		— 0.74	— 0.87	— 0.84
5.0			— 0.91	— 0.90
∞				— 0.90

Table 19.

α as function of βh and βz; $s = 0\ 9$.

βz	βh			
	0.5	2.0	5.0	∞
0.5	— 9°	— 22°	— 11°	— 10°
1.0		— 31°	— 15°	— 11°
2.0		— 35°	— 16°	— 12°
5.0			— 12°	— 2°
∞				0°

A comparison with Tables 14 and 15 shows that the effect of the turbulence is much greater for $s = 0.9$ than for $s = 0$; in Table 12 we thus find the greatest velocity for $\beta h = \beta z = 2.0$; in Table 16 for $\beta h = \beta z = 5.0$.

Complete tables have not been computed for values of s between 0 and 0.9 but it is evident that for any allowed value of s we find, that the motion varies in generally the same way as for $s = 0.9$. The most important result regarding this variation is that the maximum velocity decreases towards the bottom where it occurs at an earlier moment. Furthermore, that the configuration of the motion compared with the configuration with absence of eddy viscosity is changed in such a way, that the ellipse which represents this configuration at a short distance from the boundary surface is narrower and turned to the right of the direction of propagation instead of coinciding with that direction. If particularly βh is large the effect of the eddy viscosity is imperceptible in large distances (last columns of tables) and we find that the configuration of the motion changes in the stated, characteristic way, when approaching the bottom.

We will here confine ourselves to the statement of these results. The tables show several peculiarities which are evidently closely connected with the laws for the progress and damping of the wave but it seems unnecessary to enter upon them.

A study of the variations of the velocities within waves of different period lengths might be of interest, but would require a great amount of numerical computations and the results could at present not be applied to any observed conditions.

The mean velocity from the boundary surface to the free surface in the direction in which the wave proceeds can be expressed simply. This mean velocity is:

$$\bar{u} = \frac{1}{h}\int_0^h u\, dz\,. \tag{33}$$

We find:

$$\bar{u} = c\,\frac{\zeta_0\, e^{-\gamma x}}{h\sqrt{1+p^2}}\sin(\sigma t + \alpha - \mu x) \tag{34}$$

where

$$\operatorname{tg}\alpha = p\,. \tag{35}$$

There is consequently a phase difference between the height of the wave,

$$\zeta = \zeta_0\, e^{-\gamma x}\sin(\sigma t - \mu x)$$

and the mean velocity in the direction of progress. Since p is always positive, the maximum mean velocity always occurs *before* the maximum height is reached.

The equation:

$$\bar{u}_{max} = c\,\frac{\zeta}{h\sqrt{1+p^2}} \tag{36}$$

gives the relation between maximum mean velocity, velocity of progress, wave height and depth if the wave is damped. By absence of eddy viscosity we have $\bar{u}_{max} = u_{max}$ because u is then independent of z, furthermore, $c = \sqrt{gh}\,\frac{1}{\sqrt{1-s^2}}$ and $p = 0$ and when particularly $s = 0$ the equation (36) is reduced to the well known term:

$$u = \sqrt{\frac{g}{h}}\,\zeta\,. \tag{37}$$

It can be proved by means of the general equations in Chapter 8 that the expression for the mean velocity in the direction of progress is valid for any value of the constants of integration C_1 to C_4, and furthermore, that it is correct even if the terms for the forces of resistance, which in vector form may be written:

$$\boldsymbol{R} = \eta\,\frac{\partial^2 \boldsymbol{V}}{\partial z^2} \tag{38}$$

are replaced by a general function of the form

$$\boldsymbol{R} = f\left(\boldsymbol{V}, \frac{\partial \boldsymbol{V}}{\partial z}, \frac{\partial^2 \boldsymbol{V}}{\partial z^2}\ldots\right). \tag{39}$$

The equation (34) has, therefore, a far more general character than the equations which have elsewhere been discussed in this chapter.

11. Influence of eddy viscosity on rotary motion due to interference.

Before proceeding further, we will study the influence of the eddy viscosity on the motion in the vicinity of the bottom in the case, where the rotary character of the motion is due to interference between two waves on a resting disc. For the sake of simplicity we will assume that the waves in the point with which we deal meet at right angles and with a phase difference of $\frac{1}{4}$ period length. Furthermore, we shall suppose the depth to be so great that $e^{-\beta h}$ can be regarded as a small quantity. Placing the x- and y-axes parallel to the directions in which the waves are supposed to proceed, we then find (equations (1) Chapter 10):

$$u = \frac{g}{c}\zeta_0 e^{-\gamma x}\left[(1 - e^{-\beta z}\cos\beta z + p\, e^{-\beta z}\sin\beta z)\sin(\sigma t - \mu x) - p\left(1 - e^{-\beta z}\cos\beta z - \frac{1}{p}e^{-\beta z}\sin\beta z\right)\cos(\sigma t - \mu x)\right]$$

$$v = \frac{g}{c}\zeta_0^1 e^{-\gamma x}\left[(1 - e^{-\beta z}\cos\beta z + p\, e^{-\beta z}\sin\beta z)\cos(\sigma t - \mu x) - p\left(1 - e^{-\beta z}\cos\beta z - \frac{1}{p}e^{-\beta z}\sin\beta z\right)\sin(\sigma t - \mu x)\right] \quad (1)$$

where ζ_0 and ζ_0^1 are the amplitudes of the two waves and all other letters have their previous meaning. The equations (1) represent an ellipse for which the ratio between the axes is $\zeta_0 : \zeta_0^1$ independent of z and which for any value of z is orientated with the major axis along the x-axis or the y-axis according to the relative values of ζ_0 and ζ_0^1. The time of maximum velocity changes, however, when approaching the bottom, occurring before the corresponding velocity in great distances.

In this special case it is thus found, that the phase of maximum current is influenced in the same way as in the preceding case, when the rotary character of the motion was due to the rotation of the disc, but the configuration of the motion now remains unchanged, when approaching the bottom. This result is evidently independent of the special assumptions regarding the angle of intersection, the phase difference between the waves and the depth, because the motion must, within each wave, be modified in exactly the same way, when approaching the bottom, and the *configuration* of the combined motion due to both waves must, therefore, remain unchanged.

12. Free surface and slipping motion along the bottom.

We shall next introduce a slipping motion along the bottom, supposing that the resultant force of the resistance close to the bottom is directed against the velocity and proportional to the scalar value of the same(1). Whether this supposition is correct or not

(1) The assumption regarding the character of the resistance close to the bottom might perhaps be brought in better agreement with the actual conditions by introducing:

$$\varkappa u - \eta\frac{\partial u}{\partial z} \qquad \text{and} \qquad \varkappa v - \eta\frac{\partial v}{\partial z}$$

instead of ku and kv on the left side in equations (1). The terms $\varkappa u$ and $\varkappa v$ would then represent the direct effect of the boundary surface, the second terms the effect of the viscosity on the bottom layer. This assumption would, however, lead to complicated equations, but the character of the motion would probably not be materially altered. The terms ku and kv have been introduced with a view to future application to the tidal motion of the ice, because there are strong reasons for assuming, that the motion of the ice is subject to a resistance which is directed against the motion and proportional to the scalar value of the velocity.

has to be tested by comparing observed and theoretical results. The boundary condition for $z = 0$ now takes the form:

$$z = 0 \ , \begin{cases} \dfrac{\partial u}{\partial t} - \lambda v + k u = - g \dfrac{\partial \zeta}{\partial x} \\ \dfrac{\partial v}{\partial t} + \lambda u + k v = - 0 \end{cases} \tag{1}$$

where k means the coefficient of resistance at the bottom. To this condition we add as previously:

$$z = h \ , \ \frac{\partial u}{\partial z} = \frac{\partial v}{\partial z} = 0 \tag{2}$$

By means of the equations (1) and (2) the constants C_1 to C_4 in the equations for u and v ((15) Chapter 9) can be determined. We obtain:

$$\begin{aligned} u = & - \frac{\sigma^2}{\sigma^2 - \lambda^2} g \frac{\zeta_0}{c} e^{-\gamma x} (p + i) \left(1 - q \frac{1 - i n}{1 + n^2} \frac{\cosh (1 + i) \beta_1 (h - z)}{\cosh (1 + i) \beta_1 h} \right. \\ & \left. - r \frac{1 - i m}{1 + m^2} \frac{\cosh (1 + i) \beta_2 (h - z)}{\cosh (1 + i) \beta_2 h} \right) e^{i (\sigma t - \mu x)} \\ v = & - i \frac{\sigma^2}{\sigma^2 - \lambda^2} g \frac{\zeta_0}{c} e^{-\gamma x} (p + i) \left(\frac{\lambda}{\sigma} + q \frac{1 + i n}{1 + n^2} \frac{\cosh (1 + i) \beta_1 (h - z)}{\cosh (1 + i) \beta_1 h} \right. \\ & \left. - r \frac{1 - i m}{1 + m^2} \frac{\cosh (1 + i) \beta_2 (h - z)}{\cosh (1 + i) \beta_2 h} \right) e^{i (\sigma t - \mu x)} \end{aligned} \tag{3}$$

where

$$n = \frac{\alpha + \lambda}{k} \quad \text{and} \quad m = \frac{\alpha - \lambda}{k} \tag{4}$$

and the other letters have the same meaning as previously.

The quantities c and p are to be determined by means of the equation of continuity which leads to:

$$\begin{aligned} - \frac{\sigma^2}{\sigma^2 - \lambda^2} \cdot \frac{g h}{c^2} (p + i)^2 & \left(1 - q \cdot \frac{1 - i n}{1 + n^2} \frac{1 - i}{2 \beta_1 h} \operatorname{tgh} (1 + i) \beta_1 h \right. \\ & \left. - r \frac{1 - i m}{1 + m^2} \frac{1}{2 \beta_2 h} \operatorname{tgh} (1 + i) \beta_2 h \right) = 1 . \end{aligned} \tag{5}$$

We shall not enter upon a general discussion of these equations because no use will be made of them in the present paper. It may be sufficient to mention that the results set forth in Chapter 10 in the main are unchanged by the introduction of a slip along the bottom in this form. As previously we find, that the wave is damped and that the velocity of the wave decreases, but with a value of βh both damping and decrease of velocity are smaller than in the case we have discussed. This is evidently correct, because the assumption that no slipping motion takes place along the bottom is identical with supposing an infinite great resistance against slip, and a smaller resistance against slip now supposed must affect the wave less than an infinitely large one.

The rules for the change of the configuration of the velocities, when approaching the bottom, are in the main unaltered but modified in a way which can be shown by discussing the velocities along the bottom under various conditions.

From equations (3) we obtain for $z = 0$:

$$u_0 = \frac{\sigma^2}{\sigma^2 - \lambda^2} g \frac{\zeta_0}{c} e^{-\gamma x} [(A + p B) \sin(\sigma t - \mu x) + (-p A + B) \cos(\sigma t - \mu x)]$$
$$v_0 = \frac{\sigma^2}{\sigma^2 - \lambda^2} g \frac{\zeta_0}{c} e^{-\gamma x} [(C + p D) \cos(\sigma t - \mu x) + (p C - D) \sin(\sigma t - \mu x)] \quad (6)$$

where

$$A = 1 - q \cdot \frac{1}{1+n^2} - r \frac{1}{1+m^2}; \quad B = q \cdot \frac{n}{1+n^2} + r \frac{m}{1+m^2};$$
$$C = \frac{\lambda}{\sigma} + q \cdot \frac{1}{1+n^2} - r \frac{1}{1+m^2}; \quad D = -q \frac{n}{1+n^2} + r \frac{m}{1+m^2}. \quad (7)$$

The four coefficients A, B, C and D, according to the definition of q, r, n and m are functions of $s = \frac{\lambda}{\sigma}$ and $\frac{k}{\sigma}$ only. For any value of s can, therefore, assuming $x = 0$, the relative values $\frac{u}{F}$ and $\frac{v}{F}$, where

$$F = \frac{\sigma^2}{\sigma^2 - \lambda^2} \cdot g \frac{\zeta_0}{c} \quad (8)$$

be regarded as functions of p, $\frac{k}{\sigma}$ and t, and we can represent the configuration of the motion at the bottom by means of a set of tables similar to Tables 14 to 19.

We must, however, draw attention to the fact, that not all combinations of p and $\frac{k}{\sigma}$ are allowed. This is evident from the following considerations. By given values of k and the depth h, the damping which is proportional to p must reach the greatest possible value, when the eddy viscosity is infinitely large because then the velocities at any distance from the bottom are mostly reduced. Introducing:

$$\eta = \infty$$

we get

$$\beta h = 0$$

and the equation of continuity (5) leads to a simple expression for p by means of which the greatest possible values of p corresponding to any combination of k and s can be computed. We thus find:

Table 20.

k	p_{max}	
	$s = 0.0$	$s = 0.9$
$0.5\ \sigma$	0.24	0.66
$1.0\ \sigma$	0.42	0.66
$2.0\ \sigma$	0.62	0.67

From this it may be concluded that when assuming $s = 0$ and $k = 0.5\ \sigma$ we must assume $p < 0.24$, and so forth.

Returning to the equations (6) for the velocities along the bottom, it is seen that the motion for $s = 0$ is degenerated to an oscillation along a straight line, which may be

fully represented by means of the relative values of the maximum velocities and the phase difference expressed in degrees between these and the phase of the maximum wave height.

In Tables 21 and 22 the computed values are compiled.

Table 21.

Relative values $\frac{u_{0\,m}}{F}$ for various values of p and k.
$s = 0$.

$\frac{k}{\sigma}$	p		
	0.0	0.3	0.6
0.5	0.90		
1.0	0.70	0.74	
2.0	0.45	0.47	0.52

Table 22.

Phase differense τ_0 for various values of p and k.
$s = 0$.

$\frac{k}{\sigma}$	p		
	0.0	0.3	0.6
0.5	— 27°		
1.0	— 45°	— 29°	
2.0	— 64°	— 47°	— 33°

It may at first be noted that the tables contain no values for the combinations $k = 0.5\,\sigma$, $p = 0.3$ and $k = 0.5\,\sigma$, $1.0\,\sigma$, $p = 0.6$, because these combinations according to the previous results are self-contradictory. Furthermore, it must be emphasized, that the values within the different rows of Table 21 cannot be compared with each other, because the factor F is a function of c and dependent upon p. This does not apply to Table 22 because the factor F does not enter into the equation for τ.

The variations of $\frac{u_{0m}}{F}$ within the columns simply show that the velocities decrease with increasing resistance. From Table 22 is evident that the maximum velocity always occurs *before* the wave reaches its maximum height. The variation within the columns shows that the phase difference increases with increasing resistance but the variation within rows shows that the phase difference decreases with increasing values of p. If we especially seek the limiting values we find:

$$p = 0 \quad ; \quad \lim_{k \to \infty} \tau = -90° \tag{9}$$

$$p = 1 \quad ; \quad \lim_{k \to \infty} \tau = -45° \tag{10}$$

The first represents the case that the depth is very great, making $\beta h \to \infty$. In this case the phase of the acting force:

$$g \frac{\partial \zeta}{\partial x}$$

is 90° different from the phase of the wave, and equation (9) tells us that the phase of the velocity at the bottom coincides with the phase of the force with very great resistance. The second, on the other hand, represents the case where the damping of the wave approaches an infinitesimal large value, and then we obtain from (4) and (10), Chapter 9, that the phase difference between force and wave is $-\frac{\pi}{2} = -45°$, which means that from equation (10) we obtain again that the phase of the velocity coincides

with the phase of the force. These results are in full accordance with what might have been expected(1).

We shall next assume

$$s = 0.9$$

in which case the configuration of the motion is an ellipse, and we have in addition to the ratio $\frac{u_{0m}}{F}$ and the phase angle τ, to compute the ratio between the axes of the ellipse, r and the angle of orientation α.

The numerical values of the four quantities which characterize the motion are compiled in Tables 23 to 26. The restriction has again to be put on the values in Table 23 that the number in the rows are not comparable.

Table 23.

$\frac{u_{0m}}{F}$ as function of p and k.

$s = 0.9$.

$\frac{k}{\sigma}$	p		
	0.0	0.3	0.6
0.5	0.22	0.24	0.27
1.0	0.14	0.15	0.16
2.0	0.09	0.09	0.10

Table 24.

τ as function of p and k,

$s = 0.9$.

$\frac{k}{\sigma}$	p		
	0.0	0.3	0.6
0.5	— 47°	— 25°	— 17°
1.0	— 56°	— 38°	— 25°
2.0	— 75°	— 48°	— 34°

Table 25.

r as function of p and k.

$s = 0.9$.

$\frac{k}{\sigma}$	p		
	0.0	0.3	0.6
0.5	— 0.57	— 0.59	— 0.62
1.0	— 0.36	— 0.39	— 0.36
2.0	— 0.12	— 0.13	— 0.11

Table 26.

α as function of p and k.

$s = 0.9$.

$\frac{k}{\sigma}$	p		
	0.0	0.3	0.6
0.5	— 33°	— 33°	— 33°
1.0	— 29°	— 28°	— 28°
2.0	— 24°	— 23°	— 24°

The first two tables when compared with Tables 21 and 22 show that the velocities are more modified through the resistance on a rotating than on a resting disc, but the modifications are of the same character.

Table 25 shows that the ellipse becomes very narrow when k increases, and from Table 26 it is evident that the ellipse is turned very much to the right of the direction of progress. The greatest turning is found with the smallest value of k, but actually the turning has a maximum for a value of k between 0.3 and 0.4, and decreases towards zero when k approaches zero. It is of interest to note that both the ratio between the axes and the angle of orientation are practically independent of p, and depend upon k only within the interval here considered.

(1) Lamb, l. c. p. 544.

A comparison between Tables 23—26 and Tables 16—19 leads to the interesting result, that if the resistance close to the bottom has the character here assumed, than the configuration of the motion close to the bottom must be more changed, the ratio between the axes of the ellipse more reduced and the ellipse more turned to the right than found, assuming no slip along the bottom.

A computation of corresponding values for s between 0.0 and 0.9 gives results of the same character. A study of the variations of the configuration of the motion within waves of different period lengths will not be attempted.

The main result of the preceding discussion is, that the features which characterize the configuration of the motion in vicinity of the bottom with the presence of eddy viscosity compared with the configuration with absence of eddy viscosity, viz., the reduction of the ratio between the axes and the turning to the right of the ellipse, are intensified if it is assumed that there is a slip along the bottom, and that the resulting resistance at the bottom is directed against the velocity and proportional to the scalar value of the same. How far this supposition is correct must be tested by comparison with actually observed conditions.

13. Waves between two boundary surfaces.

Finally, we will turn to the case in which the wave proceeds between two boundaries of which the lower is supposed to be rigid and the upper of such a nature that it offers no resistance to small vertical displacements, but a considerable resistance to horizontal displacements. This case, as already mentioned, is of particular interest, because the results can be applied to the tidal wave in an ice covered, shallow sea, like the sea on the North Siberian shelf.

Regarding the law for the resistance which the upper boundary surface offers to horizontial motion, we will suppose that it is directed against the velocity and proportional to the scalar value of the same. We will, furthermore, assume that no slipping motion takes place along the upper boundary-surface, which means that the law for the motion of this surface must be valid also for the upper limit of fluid. We consequently obtain:

$$z = h \begin{cases} \dfrac{\partial u}{\partial t} - \lambda v + k_2 u = -g \dfrac{\partial \zeta}{\partial x} \\ \dfrac{\partial v}{\partial t} + \lambda u + k_2 v = 0 \end{cases}, \tag{1}$$

where k_2 means the coefficient of resistance for the upper surface.

To this condition we have to add the boundary condition at the bottom:

$$z = 0 \begin{cases} \dfrac{\partial u}{\partial t} - \lambda v + k_1 u = -g \dfrac{\partial \zeta}{\partial x} \\ \dfrac{\partial v}{\partial t} + \lambda u + k_1 v = 0 \end{cases} \tag{2}$$

which when

$$k_1 = \infty$$

has the form

$$z = 0, \qquad u = v = 0 \tag{3}$$

By means of equations (1) and (2) or (1) and (3) we can now determine the constants C_1 to C_4 in the general equations for u and v, ((15) Chapter 9) but we will make no attempt

in this direction, because the process leads to extremely complicated equations of which no practical use can be made.

We will, however, consider one special case, which at first may seem of an intricate nature, but which really is comparatively simple and represents conditions which approximately are met with in the sea.

Let us suppose that the fluid between the two surfaces consists of two distinct layers of slightly different density. The difference in density shall be so small, that we can place it out of account when developing the fundamental equations for the motion (Chapter 3), thus retaining the form of these equations unchanged, but, on the other hand, it shall be large enough to prevent any exchange of mass between the two layers of fluid. This means that the eddy viscosity is zero along the surface of discontinuity that separates the two layers. Disregarding the infinite small effect of the viscosity, we consequently find, that no tangential forces can act along this surface of discontinuity, and this leads to the condition:

$$z = h_1 , \qquad \frac{\partial u_1}{\partial z} = \frac{\partial v_1}{\partial z} = \frac{\partial u_2}{\partial z} = \frac{\partial v_2}{\partial z} = 0 \tag{4}$$

where h_1 denotes the distance of the surface of discontinuity from the bottom and the index 1 refers to the lower, the index 2 to the upper layer of the fluid.

We shall now go still one step further, and suppose that the fluid consists of 3 layers of slightly different densities. In this case we find two surfaces of discontinuity in the distances h_1 and h_2 from the bottom and at these surfaces the conditions:

$$\begin{aligned} z = h_1 , \quad & \frac{\partial u_1}{\partial z} = \frac{\partial v_1}{\partial z} = \frac{\partial u_2}{\partial z} = \frac{\partial v_2}{\partial z} = 0 \\ z = h_2 , \quad & \frac{\partial u_2}{\partial z} = \frac{\partial v_2}{\partial z} = \frac{\partial u_3}{\partial z} = \frac{\partial v_3}{\partial z} = 0 \end{aligned} \tag{5}$$

must be satisfied, where the indices 1, 2 and 3 refer to the 3 layers. The equation of continuity takes the form:

$$-\int_0^{h_1} \frac{\partial u_1}{\partial x} dz - \int_{h_1}^{h_2} \frac{\partial u_2}{\partial x} dz - \int_{h_2}^{h} \frac{\partial u_3}{\partial x} dz = \frac{\partial \zeta}{\partial t} . \tag{6}$$

The eddy viscosity may have different but constant values within each layer.

The velocities can then in each layer be represented by the general equations (14), Chapter 9 in which the constants C_1 to C_4 must now be determined by means of the boundary conditions for each layer. For the middle layer we obtain directly by means of (5):

$$C_1 = C_2 = C_3 = C_4 = 0 ,$$

which gives:

$$\begin{aligned} u_2 &= \frac{\sigma^2}{\sigma^2 - \lambda^2} g \frac{\zeta_0}{c} e^{-\gamma x} [\sin(\sigma t - \mu x) - p \cos(\sigma t - \mu x)] \\ v_2 &= \frac{\lambda}{\sigma} \frac{\sigma^2}{\sigma^2 - \lambda^2} g \frac{\zeta_0}{c} e^{-\gamma x} [p \sin(\sigma t - \mu x) + \cos(\sigma t - \mu x)] . \end{aligned} \tag{7}$$

As conditions which are to be fulfilled at the boundaries, we shall introduce:

$$k_1 = k_2 = \infty$$

or

$$z = 0 \quad , \quad u_1 = v_1 = 0 \quad ; \quad z = h \quad , \quad u_3 = v_3 = 0 \tag{8}$$

The velocities in the lower and upper layer can then be represented by equations of the same form as equations (3), Chapter 10:

$$\begin{aligned} u_1 &= \frac{\sigma^2}{\sigma^2 - \lambda^2} \frac{g}{c} \zeta_0 e^{-\gamma x} [M_1 \cos(\sigma t - \mu x) + N_1 \sin(\sigma t - \mu x)] \\ v_1 &= \frac{\lambda}{\sigma} \frac{\sigma^2}{\sigma^2 - \lambda^2} \frac{g}{c} \zeta_0 e^{-\gamma x} [P_1 \cos(\sigma t - \mu x) + Q_1 \sin(\sigma t - \mu x)] \end{aligned} \tag{9}$$

and

$$\begin{aligned} u_3 &= \frac{\sigma^2}{\sigma^2 - \lambda^2} \frac{g}{c} \zeta_0 e^{-\gamma x} [M_2 \cos(\sigma t - \mu x) + N_2 \sin(\sigma t - \mu x)] \\ v_3 &= \frac{\lambda}{\sigma} \frac{\sigma^2}{\sigma^2 - \lambda^2} \frac{g}{c} \zeta_0 e^{-\gamma x} [P_2 \cos(\sigma t - \mu x) + Q_2 \sin(\sigma t - \mu x)] \end{aligned} \tag{10}$$

where the significance of M_1 to Q_2 is evident by comparison with equations (3), Chapter 10. Writing the equations thus, we have in the last equations, referring to the upper layer, transferred the origin to the upper surface and inverted the direction of the positive z-axis.

Expressing the thickness of the different layers in fractions of the total depth, h,

$$h_1 = d_1 h \quad , \quad h_2 = d_2 h \quad , \quad h_3 = d_3 h$$

we obtain from the equation of continuity (6):

$$2p(d_1 S_1 + d_2 + d_3 S_3) + (p^2 - 1)(d_1 T_1 + d_3 T_3) = 0 \tag{11}$$

$$\frac{\sigma^2}{\sigma^2 - \lambda^2} \frac{gh}{c^2} [(1 - p^2)(d_1 S_1 + d_2 + d_3 S_3) + 2p(d_1 T_1 + d_3 T_3)] = 1 \tag{12}$$

where the meaning of the terms S_1 to T_3 is evident by a comparison with equations (7) to (10), Chapter 10.

The equations (7) and (9) to (12) represent a complete solution of the present problem.

Before illustrating the content of the equations (7) to (12) by means of an numerical example, we may draw a few general conclusions from them.

The motion of the middle layer is always very simple. The velocities are independent of z and can be expressed in the form:

$$\begin{aligned} u_2 &= F\sqrt{1 + p^2} \sin(\sigma t + \alpha - \mu x) \\ v_2 &= \frac{\lambda}{\sigma} F\sqrt{1 + p^2} \cos(\sigma t + \alpha - \mu x) \end{aligned} \tag{13}$$

where

$$\operatorname{tg} \alpha = p \tag{14}$$

From these equations is evident that the configuration of the motion is represented by an ellipse with the major axis

$$u_{max} = F\sqrt{1+p^2} = \frac{\sigma^2}{\sigma^2 - \lambda^2} \frac{g \zeta_0 e^{-\gamma x}}{c} \sqrt{1 + p^2} \tag{15}$$

This maximum velocity is always greater than the maximum velocities in a wave of the same height with absence of eddy viscosity because c is always smaller than c_0, the velocity of progress of an undisturbed wave, and because the factor $\sqrt{1 + p^2}$ always is greater

than 1. Furthermore, it is seen that the ratio between the axes of the ellipse is normal, $r = \frac{\lambda}{\sigma}$, and that the ellipse is orientated with the major axis coinciding with the direction of progress of the wave, but the maximum current occurs after the wave has passed the maximum height, the difference expressed in degrees is:

$$\tau = \text{arctg}\, a\,.$$

We have here assumed p to be different from zero.

If, however, $(\beta h)_1 = (\beta h)_3 = 0$, which may take place when $\eta_1 = \eta_3 \to \infty$, we have

$$S_1 = S_2 = T_1 = T_2 = 0 \tag{16}$$

and equation (11) and (12) are reduced to

$$\begin{aligned} p &= 0 \\ c^2 &= gh\, d_2 \cdot \frac{\sigma^2}{\sigma^2 - \lambda^2} \end{aligned} \tag{17}$$

Equations (7) can then be written

$$\begin{aligned} u &= \sqrt{\frac{\sigma^2}{\sigma^2 - \lambda^2}} \cdot \frac{g\,\zeta_0}{\sqrt{gh\, d_2}}\, e^{-\gamma x} \sin(\sigma t - \mu x) \\ v &= \frac{\lambda}{\sigma} \sqrt{\frac{\sigma^2}{\sigma^2 - \lambda^2}} \cdot \frac{g\,\zeta_0}{\sqrt{gh\, d_2}}\, e^{-\gamma x} \cos(\sigma t - \mu x) \end{aligned} \tag{18}$$

These equations evidently express that the wave now proceeds within the middle layer as if the two other layers did not exist.

As numerical values, with future application in view, we will introduce

$$\begin{aligned} &\frac{\lambda}{\sigma} = 0.9 \quad , \quad (\beta h)_1 = 3.0 \quad , \quad (\beta h)_3 = 1.0 \\ &d_1 = 0.245 \quad , \quad d_2 = 0.090 \quad , \quad d_3 = 0.665 \end{aligned} \tag{19}$$

The equation of continuity then gives

$$p = 0.35 \quad , \quad c = \sqrt{gh}\ 1.20 \tag{20}$$

Introducing the values for $\frac{\lambda}{\sigma}$ and c in the equations for u and v, these can be written:

$$\begin{aligned} u &= 4.39 \frac{\zeta}{\sqrt{gh}} [M \cos(\sigma t - \mu x) + N \sin(\sigma t - \mu x)] \\ v &= 3.95 \frac{\zeta}{\sqrt{gh}} [P \cos(\sigma t - \mu x) + Q \sin(\sigma t - \mu x)] \end{aligned}$$

and we can consequently compute relative values of the velocities in various depths without any assumption regarding h and ζ.

We can again characterize the motion in various depths by means of the relative values of the maximum velocities, $V \cdot \frac{\sqrt{gh}}{\zeta}$, the phase difference between maximum velocity and wave height, the ratio between the minimum and maximum velocities indicating the direction in which the velocities rotate by the sign, and the angle between the direction of maximum velocity and direction of progress.

In Table 27 the values for 5 depths are compiled. The two upper rows refer to the motion of the upper layer; the middle row to the middle layer, and the two lowest rows to the motion of the bottom layer.

Table 27. Example of velocities in a wave propagating between two boundaries in a fluid of varying density.

$\frac{z}{h}$	$V.\frac{\sqrt{gh}}{\zeta}$	τ	r	α
0.7	0.55	— 39°	— 0.11	— 25°
0.5	0.61	— 37°	— 0.27	— 27°
0.3	4.66	+ 20°	— 0.90	0°
0.2	3.32	— 7°	— 0.86	— 30°
0.1	2.32	— 17°	— 0.80	— 22°

In the upper layer, the maximum velocities are very small, they occur before the wave reaches its maximum height, and the configuration of the motion is represented by a narrow ellipse, turned to the right.

In the middle layer, we find very large velocities but the maximum velocity is here reached *after* the wave height has passed the greatest value. It is of interest to note that the maximum velocities in a wave of the same height propagating in a layer of fluid of the same depth by absence of eddy-viscosity had been only $2.29 \cdot \frac{\zeta}{\sqrt{gh}}$, less than half of the value met with in the middle layer. The form and the orientation of the ellipse representing the configuration of the motion had, however, been the same.

In the bottom layer, we finally find smaller velocities occurring too early and configurations represented by ellipses which are too narrow and turned to the right relative to the ellipse of the middle layer.

The example here discussed may be regarded as a step towards a study of the motion, when the eddy viscosity varies with the depth. From the results we may conclude that in this case we may encounter very complicated motions, but that the rules we have previously found for the modification of the motion in the vicinity of a boundary-surface remain unaltered.

14. The energy of the wave.

We may, as previously, define the mean energy of a column of water during one period as

$$\bar{E} = \frac{1}{T}\int_0^h\int_0^T E_p \, dz \, dt + \frac{1}{T}\int_0^h\int_0^T E_k \, dz \, dt \tag{1}$$

where E_p denotes the potential and E_k the kinetic energy of a unit of volume. By absence of turbulense and viscosity is

$$\bar{E}_p = \frac{1}{4} g\varrho\,\zeta^2 \quad , \quad \bar{E}_k = \frac{1}{4} g\varrho\,\zeta^2 \frac{\sigma^2 + \lambda^2}{\sigma^2 - \lambda^2} \tag{2}$$

On a resting plane, $\lambda = 0$, the mean kinetic energy is equal to the mean potential energy, on a rotating disc it is always greater. Only the kinetic energy is subject to dissipation through the eddy viscosity, and accordingly we have found that the effect of the eddy viscosity on the velocity of progress and the damping of the wave and on the velocities of the particles of fluid is much greater on a rotating than on a resting disc.

The expression for the potential energy remains unchanged with the presence of eddy viscosity but the expression for the kinetic energy is evidently changed because the velocities are function of the distance from the boundary surface.

The simple relation between the mean kinetic and the mean potential energy

$$\bar{E}_k = \bar{E}_p \cdot \frac{\sigma^2 + \lambda^2}{\sigma^2 - \lambda^2} \tag{3}$$

is, therefore, no longer valid with the presence of eddy viscosity but a derivation of the exact equations for this relation leads to very complicated equations. Only in one case is a simple relation found.

Assuming

$$\lambda = 0$$

and

$$z = 0 \quad , \quad u = 0 \quad , \quad e^{-\beta h} = \varepsilon$$

where ε is a small quantity which may be omitted, we obtain by means of equations (3) p. 14:

$$\bar{E}_k = \frac{1}{2}\frac{1}{T}\int_0^h\int_0^T \varrho\, u^2\, dz = \bar{E}_p \cdot \frac{1-p^2}{1+p^2} \tag{4}$$

where p has the same meaning as previously.

From equation (4) it is seen, that the mean kinetic energy of a wave on a resting disc with presence of eddy-viscosity is always smaller than the potential, assuming βh to be great. The same rule is evidently correct even with small values of βh. In the case $\beta h = 0.5$, we find, for instance by means of the numerical values upon which Table 14 is based, that:

$$E_k = 0.21\, E_p .$$

On a rotating disc it is correspondingly found, that the mean kinetic energy with presence of eddy viscosity is smaller than with its absence, but it may nevertheless be greater than the potential energy. We may compute numerical values of E_k for $\frac{\lambda}{\sigma} = 0.9$ and the values of βh used in Tables 16 to 19. We have

$$\bar{E}_k = \frac{1}{2}\frac{1}{T}\int_0^h\int_0^T \varrho\,(u^2 + v^2)\, dz\, dt$$

and obtain by introducing u and v from equation (26), Chapter 10, and the value of c from (20):

$$\bar{E}_k = \bar{E}_p \frac{1}{w^2}\frac{\sigma^2}{\sigma^2 - \lambda^2}\frac{1}{h}\int_0^h (M^2 + N^2 + P^2 + Q^2)\, dz . \tag{5}$$

Using the values of M, N, P and Q upon which Tables 16 to 19 have been based, we find

Table 28. $\frac{\lambda}{\sigma} = 0.9$.

βh	$\frac{E_k}{E_p}$	$\frac{E_k}{E_p} \cdot \frac{\sigma^2 - \lambda^2}{\sigma^2 + \lambda^2}$
∞	9.5	1.00
5.0	8.55	0.90
2.0	3.0	0.31
0.5	0.20	0.02

The first row in the table, $\beta h = \infty$, corresponds to $\eta = 0$ or absence of eddy viscosity. The first column contains the ratio between the kinetic and potential energy, the second contains the kinetic energy expressed in fractions of the corresponding kinetic energy with absence of eddy viscosity, which we may call the normal value.

We find that in the special cases here considered the kinetic energy with presence of eddy viscosity is always smaller than normal.

It is probably possible to show that this rule has a general character, independent of the special assumptions regarding the nature of the eddy viscosity on which the numerical values in the table are based. The writer has, however, not succeeded in formulating the general considerations in clear words and will, therefore, refrain from entering upon them.

When the velocities and the boundary conditions are known the mean dissipation of the energy in a column of fluid can be computed by means of the function of dissipation which when all terms of small order are omitted is reduced to

$$\bar{F} = \frac{1}{T} \int_0^h \int_0^T \eta \left[\left(\frac{\partial u}{\partial z} \right)^2 + \left(\frac{\partial v}{\partial z} \right)^2 \right] dz\, dt \tag{6}$$

In case $\lambda = 0$, $e^{-\beta h} = \varepsilon$ and $z = 0$, $u = 0$, $z = h$, $\frac{\partial u}{\partial z} = 0$ is:

$$\bar{F} = \frac{g^2 \zeta^2}{c^2} (1 + p^2) \sqrt{2 \eta \sigma} \tag{7}$$

In the general case is the corresponding expression very complicated.

A formula which may be of value for numerical computations can be derived from the equations for u and v (26), Chapter 10. We find

$$\bar{F} = \frac{1}{2} \left(\frac{\sigma^2}{\sigma^2 - \lambda^2} \right)^2 \frac{g^2 \zeta_0^2}{c^2} \int_0^h \eta \left[\left(\frac{\partial M}{\partial z} \right)^2 + \left(\frac{\partial N}{\partial z} \right)^2 + \left(\frac{\partial P}{\partial z} \right)^2 + \left(\frac{\partial Q}{\partial z} \right)^2 \right] dz \tag{8}$$

This formula may be useful if the dissipation of the energy due to «tidal friction» shall be computed from current observations, but no attempts in this direction will be made in the present paper.

IV. Application of theoretical Results.

15. Summary of Results.

In the preceding chapters long, gravitational waves in a homogeneous, non-viscous, rotating fluid have been studied in two cases, namely, in a layer of even depth, in an infinitely long rotating channel (Lord Kelvin), and on an unlimited, rotating disc.

In a channel, long waves of all period lengths are possible. The laws for the motion of the particles of fluid and the velocity of progress of the wave are the same as for waves in a non-rotating channel (Fig. 6). The motion of the particles of fluid alternates

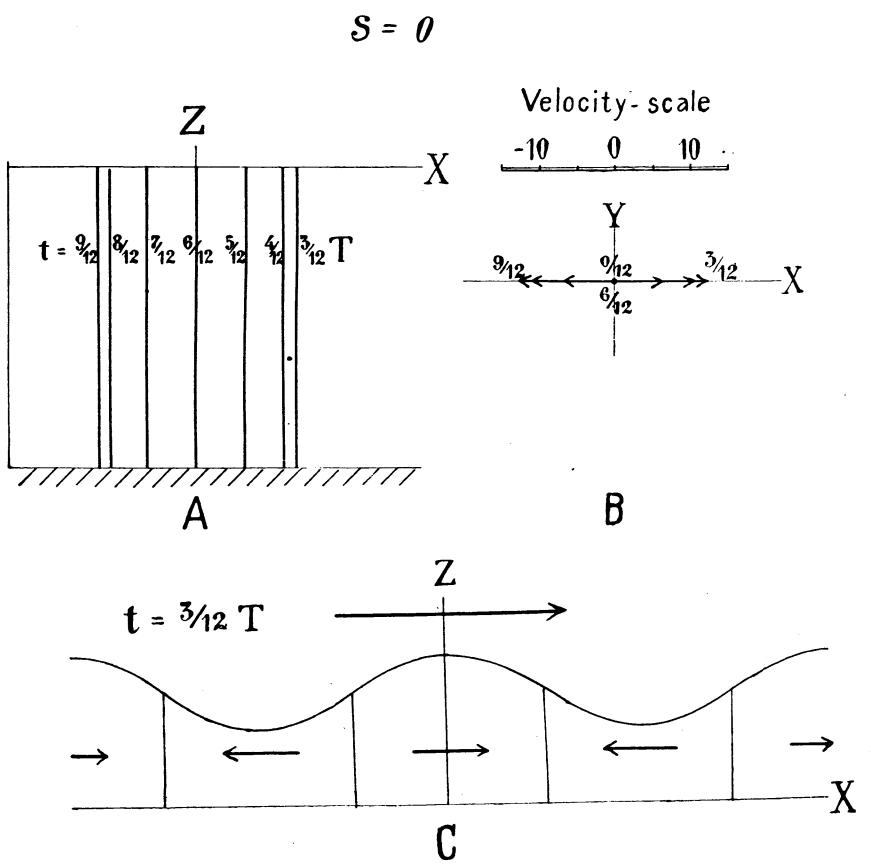

Fig. 6.

in the direction or against the direction of progress. The maximum velocity occurs when the wave reaches maximum height, and supposing the constant of gravity to be invariable, depends solely upon the amplitude of the wave and the depth. The motion is uniform from the bottom to the surface. The velocity with which the wave proceeds depends only upon the depth. Half the energy of wave is present as kinetic, half as potential energy. The wave differs, however, from a corresponding wave in a non-rotating channel by the circumstance, that the amplitude of the wave varies across a section of the channel, decreasing from right to left, referred to the direction in which the wave proceeds if the rotation is counter-clockwise and from left to right if clockwise. The effect of the

forces of inertia arising from the rotation is to press the wave to the right of the channel by counter-clockwise rotation, to the left by clockwise.

In a layer of fluid of constant depth on an unlimited, rotating disc progressive wave of the kind here studied are possible only when the period length of the wave is shorter than half the time required by the disc for one revolution. This condition can conveniently be written $s < 1$ where s is the ratio between the named quantities (Fig. 7).

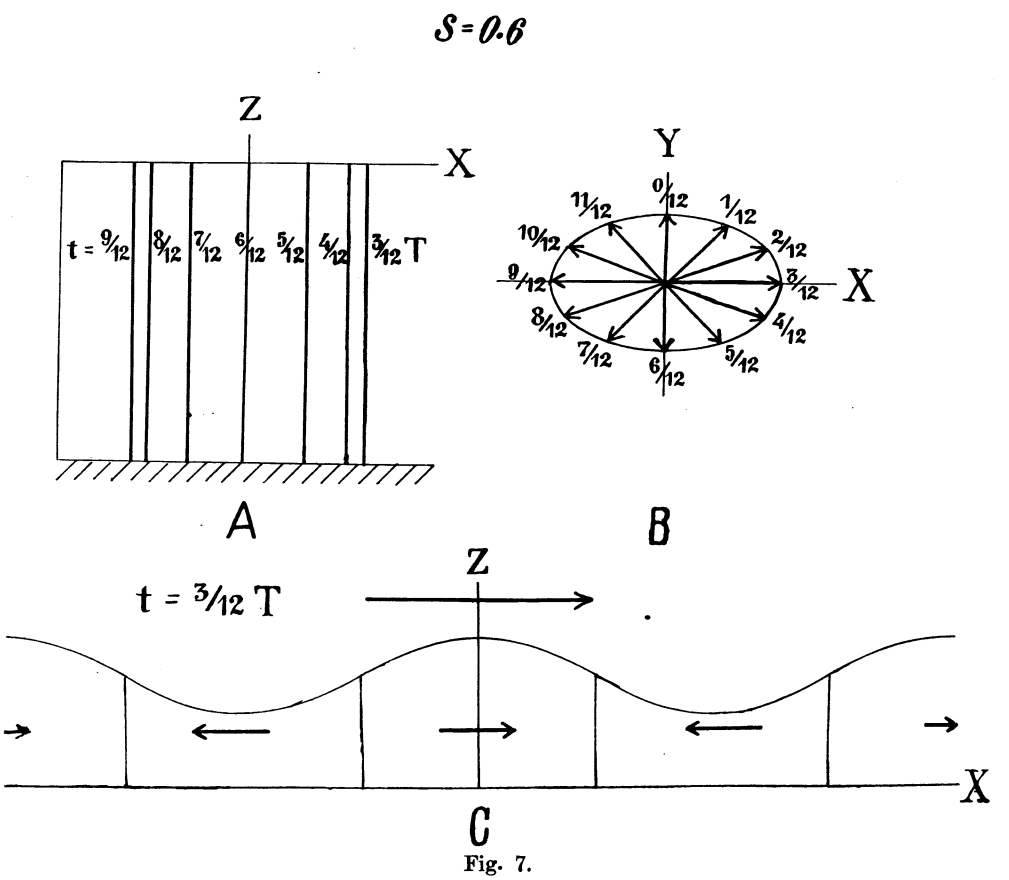

Fig. 7.

The motion of the particles of fluid is not alternating but rotates clockwise if the disc rotates counter-clockwise, and vice versa. If the velocities during one period are represented by a central vector diagram the end points of the vectors describe an ellipse. The maximum velocity occurs when the wave reaches its maximum height, and is large compared with the amplitude of the wave. It now depends not only upon the amplitude of the wave and the depth, but also upon the ratio s, approaching infinite values, when s approaches 1, provided the amplitude remains finite. The direction of the maximum velocity coincides with the direction in which the wave proceeds. The ratio between minimum and maximum velocity and the motion is uniform from the bottom to the surface and is equal to s. The wave proceeds with a velocity which depends not only upon the depth, but also upon the ratio s, increasing towards infinite values, when s approaches 1. The amplitude of the wave is constant along the wave front, but must, if the energy of the wave shall remain constant, decrease by increasing velocity of rotation. The effect of the forces of inertia is now to preserve the major part of the energy of the wave as kinetic energy.

A formal solution, which refers to no defined boundary-conditions, represents an intermediate case in which the motion is rotary but the ratio between minimum and

maximum velocity is smaller than s and the amplitude of the wave decreases from right to left if the disc rotates counter-clockwise.

The resistance modifies these laws to a great extent. The resistance influences primarily the layer close to the bottom, but by the eddy viscosity is transferred to a great distance from the latter. Supposing the eddy viscosity to be constant the dynamic equations have been solved for waves on an unlimited, rotating disc, but not for waves in a rotating channel. All the following rules apply, therefore, to waves on an unlimited disc. (Fig. 8).

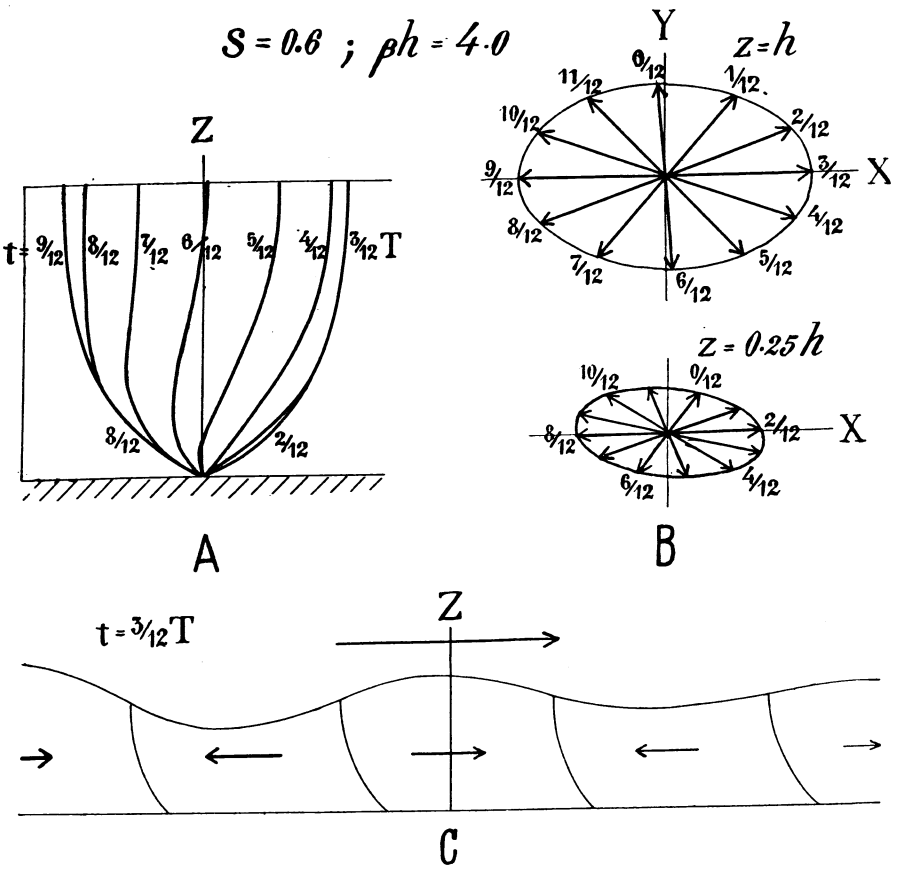

Fig. 8.

Where the influence of the resistance is perceptible the motion of the particles of fluid is generally so modified that the maximum velocity occurs before the wave reaches its maximum height and is directed to the right, when referred to the direction in which the wave proceeds if the disc rotates counter-clockwise, to the left if clockwise. The motion is still rotary, but the ratio between minimum and maximum velocity is smaller than with absence of resistance. In a wave proceeding in a fluid with a free upper surface and of sufficient depth, the laws for the motion of the particles of fluid at the surface are practically the same as with absence of resistance. In this case it is found, that the character of the motions changes in a marked way when approaching the bottom. The maximum velocity occurs earlier, and supposing the rotation of the disc to be counter-clockwise, is turned to the right referred to the corresponding velocity in the upper layer, and the ratio between minimum and maximum velocity decreases.

If, on the other hand, the rotary motion is due to interference between two waves on a resting disc, it is found that the maximum velocity close to the bottom occurs earlier

than in the upper layer, but that the direction is the same, and the ratio between minimum and maximum velocity remains unchanged.

The modifications of the velocities of the particles of fluid within a wave which proceeds between two boundary surfaces of which the upper offers no resistance to vertical displacements has been studied in one case. We shall later return to the results of the investigation which find application under special conditions.

The velocity of progress is diminished by the resistance. The reduction depends, supposing the rotation of the disc, the depth and the eddy viscosity to be constant, on the period length of the wave. Generally the velocity of progress of the longest waves is mostly reduced, but the laws are too complicated to be entered upon in detail.

The amplitude of the wave decreases in the direction in which the wave proceeds. This damping of the wave depends upon the period length of the wave, and generally the shorter waves are more reduced on a given distance than the longer, but this rule is not valid under all conditions.

16. General applications to the tidal phenomena.

The above results refer to free, progressive waves, and can, therefore, only be applied to the tidal phenomena within regions where the tidal waves, which are produced directly by the action of the tidal forces, are negligible compared with the waves entering these regions, and proceeding across them. As such regions particularly the continental shelves come into consideration(1), in the application it must, however, be remembered, that the actual conditions deviate more or less from the conditions which were supposed when deriving the theoretical results. We shall briefly discuss the restrictions which arise from the discrepancies.

1. The fluid has been supposed to be homogeneous. The non-homogeneity of the seawater is of no importance, because the variations of the density are small when compared with the density itself. It is generally assumed that the non-homogeneity can be disregarded when dealing with waves of the kind here treated.

2. The depth is supposed to be constant. The deviations from constant depth may modify the wave, but it is generally assumed that it is permissible to introduce an average depth and regard this as constant.

3. Our results refer to waves on a rotating disc, but we wish to apply them to waves on a rotating sphere. This is approximately correct, if the applications are confined to regions within which

$$\lambda = 2\,\omega\,\sin\varphi$$

may be regarded as constant. Here ω means the angular velocity of the earth's rotation and φ the geographical latitude.

4. The waves have been supposed to proceed in an infinite long channel or on an unlimited disc, but the continental shelves represent limited regions. The modifications which arise from the boundary conditions are undoubtedly of great importance and will be more fully discussed later.

5. The eddy viscosity has supposed to be constant. This supposition represents a very rough approximation to the actual conditions, but variations of the eddy viscosity cannot be expected to change the character of the modifications due to the resistance.

In view of the great differences between the supposed and the actual conditions, we cannot expect that the theoretical results indicate more than the general lines which the modifications due to the rotations of the earth and the resistance follow. The

(1) Krümmel l. c.

deflecting force of the earth's rotation is zero at the equator and greatest at the poles, for which reason the effect of the rotation must increase towards the poles. The resistance is evidently of importance in any latitude, but we have found that waves on a rotating disc are more affected by the resistance, than corresponding waves on a resting disc, and must therefore expect the effect of the resistance to increase from the equator to the poles.

We will at first regard the tidal wave as a simple wave, e. g. a wave which can be represented by a single harmonic function, with a period length of 12.4 hours and discuss the modifications of the tidal currents, the rate of progress, and the range of the tide.

1. *Tidal currents.* We must expect that the tidal currents on an open continental shelf, across which the wave proceeds towards the coast, rotate clockwise on the northern and counter-clockwise on the southern hemisphere, and alternate in the equatorial regions. The current measurements, which at present are known to the writer, are all from the northern hemisphere, where it is generally found that the tidal currents off the coasts rotate clockwise. In a few regions counter-clockwise rotating currents have been encountered and explained by interference, but the circumstance that the clockwise rotating currents are by far the more frequent, indicates that the rotary character must generally be due to the deflecting force of the earth's rotation and not to interference. In order to decide whether the rotary currents within a certain region are caused by interference or are due to the rotation of the earth, extensive current observation are necessary, but important conclusions can also be drawn from observations of the tidal currents in various depths at a single station because the currents must change in different ways, when approaching the bottom according to the circumstances which are responsible for the rotating character. An example from the North Sea, that may be used to illustrate this, is found in Helland-Hansen's paper «Current-measurements in 1906»(1), containing current observations during 13 hours at Ling Bank, Lat. 58° 17′ North, Long. 2° 27′ East, taken August 7 and 8, 1906, in the depths 2, 5, 10, 20, 50 and 75 meters. The depth was at this station 80 meters. Helland-Hansen found that the tidal currents in the two lowest depths, 50 and 75 meters were characterized by being weaker and reaching their maximum values an hour earlier than the tidal currents in the upper strata. Furthermore, that the direction of the maximum velocity was turned to the right referred to the corresponding direction in the upper strata, and that the ratio between minimum and maximum current was decreasing towards the bottom. These features are clearly evident from the central vector diagrams in Fig. 9 which are copies of the representations of the original observations, published in Helland-Hansen's paper. Helland-Hansen draws attention to them and suggests that they may be due to a tidal wave reflected from the West Coast of Norway and proceeding into the North Sea into the deeper strata. The observed changes are, however, in agreement with the results which were summarized in the preceding chapter, for which reason it seems more probable that they simply indicate the influence of the resistance along the bottom on the tidal currents, in a single wave which has been modified by the earth's rotation. This isolated example can, however, hardly be regarded as a sufficient proof for this conception.

If the rotary currents are fully developed the ratio between minimum and maximum velocity according to the theory is to be

$$s = \frac{\lambda}{\sigma} = \frac{2\omega \sin\varphi}{2\pi} \cdot T$$

(1) Bergens museums aarbog 1907, No. 15.

where T is the period length of the wave. Introducing $T = 12.4$ hours and $\omega = 2\pi : 24$, expressing the time which the earth uses for one revolution in hours, we find

$$s = \sin\varphi \cdot \frac{12.4}{12} \cdot 1.033 \sin\varphi$$

We must expect, however, that the observed ratio between the minimum and maximum current is generally smaller because the coasts in most cases prevent the full development of the rotary currents. In above example is $\varphi = 58°.3$, making

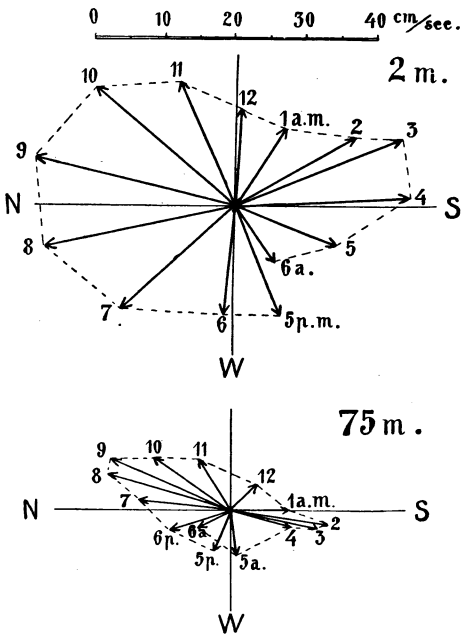

Fig. 9. Currents on Ling Bank, Aug. 7 and 8, 1906.

$$s = 0.88$$

but the observations from 2 meters give a considerably smaller value, which shall be called r, namely

$$r = 0.55.$$

2. *Rate of progress.* When the tidal currents are rotary the wave must be expected to progress with a velocity, which is greater than the «normal» velocity $c = \sqrt{gh}$. On an unlimited, rotating disc a wave with absence of resistance proceeds with the velocity

$$c = \sqrt{gh} \cdot \sqrt{\frac{1}{1 - s^2}}$$

but this equation, when applied to conditions on the earth, can only then be approximately correct, when the rotary currents are fully developed so that the ratio between the minimum and maximum current is equal to s. If the full development is prevented by coasts, the velocity of progress must be smaller. In this case it seems reasonable to assume, that the conditions approximately correspond to the intermediate case, dealt with in Chapter 7 according to which the velocity of progress is

$$c = \sqrt{gh} \sqrt{\frac{1 - r^2}{(1 - sr)^2}}$$

where s means the theoretical ratio between the minimum and maximum current, in this case $s = 1.033 \sin\varphi$, and r denotes the observed ratio.

The resistance must diminish the velocity of progress. This may nevertheless exceed the normal value $\sqrt{gh}$ if the rotary currents are well developed, but may decrease beyond this value if the currents are practically alternating.

3. *The range of the tide.* Regarding the range of the tidal wave within a given region a few general conclusions can be drawn. If the tidal currents are rotary the range must be expected to be small compared with the velocity of the tidal currents. If the rotary character is fully developed the range must remain constant along the wave front (along the cotidal lines), but if the full development is prevented by coasts the range must decrease from right to left on the northern hemisphere referred to an observer looking in the direction in which the wave proceeds, from left to right on the southern hemisphere.

The resistance must cause the range to decrease in the direction in which the wave proceeds, but this decrease may be entirely eliminated by convergencies due to the form of the coast. One consequence of the damping, however, is that the range of the tide at the inner part of a basin must be smaller than computed from the range at the outer part of the basin, considering the form and depth of the basin.

4. *Influence of coasts.* The coasts must modify the tidal wave very much, because, as frequently mentioned, they prevent the free development of the rotary currents. It is impossible to discuss the influence of the coasts in any exhaustive way, but a few examples may indicate the general lines which these modifications may be expected to follow. These examples refer to conditions on the northern hemisphere, and if they are to be applied to conditions on the southern hemisphere must «right» be replaced by «left», and vice versa.

We shall at first assume that the coast line runs perpendicular to the direction in. which the wave proceeds (Fig. 10). In this case no great modifications are to be expected. The rotary currents can be developed close to the coast, with the consequense that the tidal currents off the coast must be expected to run not only towards but also parallel to the latter. The range of the tide must be small compared with the velocity of the tidal currents at some distance from the coast, and the wave must approach the coast with a speed which exceeds the normal value $\sqrt{gh}$. The latter rules may, however, be modified by the influence of the resistance.

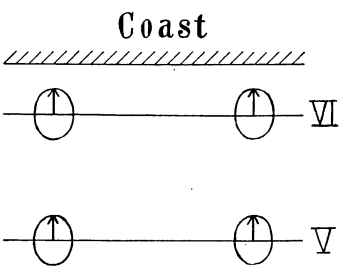

Fig. 10. Wave proceeding towards a coast.

We will next assume that a coast line runs in the direction in which the wave proceeds, and on the right hand of an observer, looking in that direction. For the sake of simplicity the depth shall be supposed to be constant. In this case the development of the rotary currents is prevented along the coast but they may exist at greater distances, as indicated in Fig. 11. At the coast, where the tidal currents are alternating, the deflecting force of the earth's rotation must be counter-balanced by a slope of the wave crest which at highwater is directed towards the coast, at low-water from the coast. This implies, that the range of the tide must decrease when departing from the coast, in other words, the deflecting force presses the wave towards the coast. Close to the latter the range must be expected to decrease approximately according to the law which Lord Kelvin found for the change in range across a channel, because the tidal currents have the same character as in a channel.

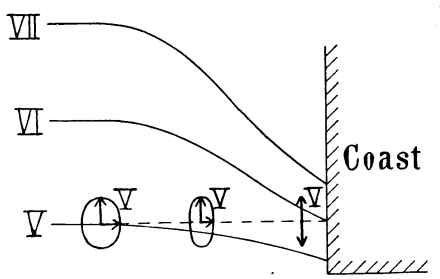

Fig. 11. Wave with a coast on the right side.

In addition to this primary effect of the deflecting force a secondary comes, which has the result, that the time of highwater at the coast does not correspond exactly to the time of max. current. Let us assume that the maximum tidal currents occur simultaneously at for instance V hours, Gr. lunar time at a series of stations lying on a straight line perpendicular to the coast, the stippled line in Fig. 11. The outer station is supposed to be so far removed from the coast, that the rotary currents here are fully developed. At this station, therefore, the conditions must be regarded as undisturbed and the time of highwater must coincide with the time of maximum current. The cotidal line V consequently passes through this station. Between high and lowwater at this stations, as indicated on the figure, the currents now run towards the coast. These

currents must continue to press the water towards the coast after highwater should have been passed, making the highwater at the coast occur after highwater at the outer station in spite of the max. currents occurring simultaneously. The cotidal line V must, therefore, have a course as shown in the figure. The rate with which the wave proceeds, increases when departing from the coast, corresponding to the development of the rotary currents, giving the cotidal lines the curved forms which are indicated by the lines VI and VII in the figure. The conditions which are here supposed can evidently exist only along a coast line, which is short compared with the wave length because the direction of the wave front is changing.

The effect of a coast on the left side of the wave is more difficult to overlook (Fig. 12). The primary effect is evidently to press the wave away from the coast, but the secondary effect, due to the convergence towards the coast of the transversal currents, is to press the wave against the coast *before* highwater is reached at the outer station, because the currents run towards the coast between low and highwater at the outer station. Whether the effect of the convergence is large enough to convert the increase of the range which should otherwise be expected when departing from the coast, cannot be decided, but it must have the result that highwater at the coast now occurs before the time of maximum current under the conditions supposed in Fig. 12. The cotidal line V must be curved as shown in the Fig. 12, and since the rate of progress increases when departing from the coast, the next cotidal lines VI and VII must approximately appear as indicated.

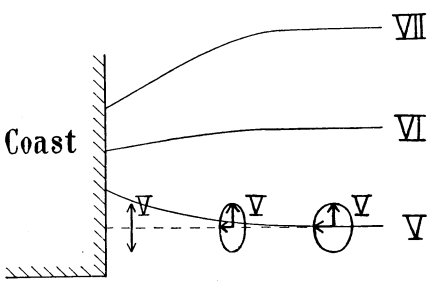

Fig. 12. Wave with a coast on the left side.

These examples can only serve to show the modifications, which may be expected under the particular conditions supposed. If corresponding considerations are to be applied in a special case, the supposed conditions must be made to agree approximately with the actual ones. From the examples, however, the general conclusion can be drawn, that the range of the tide must be expected to be great along a coast lying on the right side of the wave, but small along a coast on the left side. This conclusion is in agreement with the experience which Krümmel(1) emphasizes in the words: «When two or more waves, proceeding in different directions, meet, the rotation of the earth enters in a very remarkable way by always favouring amongst the competitors the wave which has the coast line to the right and making this wave dominating for the highwater intervals».

In a channel where no rotary currents can be developed the conditions are simpler. According to Lord Kelvin's results the wave must proceed with normal velocity, but the range must decrease from the right to the left side. Lord Kelvin's results have already found applications in so many well known cases, that it seems unnecessary to enter upon them here.

We shall presently, when returning to the tidal wave on the North-Siberian shelf, find applications for all the above conclusions regarding the modifications of the tidal currents, the velocity of progress, and the range of the tidal wave, which appear as the combined effect of the deflecting force, the resistance, and the coasts. Whether other applications can be found remains to be examined.

We have up to now regarded the tidal wave as a simple wave with a period length of 12.4 hours. Actually, however, the tidal wave is regarded as composed of a number of partial waves of various period length, of which the most important are

(1) L. c.

Symbol	Period length hours
S_2	12.00
M_2	12.42
N_2	12.66
K_1	23.93
O_1	25.82

The quality of the tide is at any station characterized by the ratios between the amplitudes of the different partial waves and the phase differences between them. We have found that the effects of the deflecting force and the resistance depend upon the period length of the wave and must therefore expect that the different partial waves are modified in different ways. This evidently leads to the conclusion that the quality of the tide must change within every region. Within the known regions, the quality of the tides is actually subject to numerous changes which have only partly been explained. Whether some of these changes can be referred to the influence of the earth's rotation and the resistance, can only be decided by a close inspection of extensive observations, and in this place, therefore, only a single feature will be mentioned.

We have found, that the shorter waves are generally more rapidly damped by the resistance than the longer. One consequence of this is that in the inner parts of shelves and shallow bays the longperiodic waves must be expected to be more dominating than in the outer parts. An examination of the informations compiled by Krümmel seems to confirm this conclusion. The ratio between the amplitudes of the daily and the half-daily tidal waves increases frequently towards the inner parts of bays and shelves, indicating that the longer waves are relatively higher in these parts. The most marked increase of the daily index is found in the Java Sea, but seems there to be far to great to be explained as resulting from the selective action of the resistance, but in several other cases this action may perhaps have to be considered. As examples the values in Table 29 have been compiled. A thorough examination of all available data from these regions would, however, be required in order to decide the question.

Table 29.

Region	Station	$\frac{K_1 + O_1}{S_2 + M_2}$
South American shelf	Montevideo	0.30
	Buenos Aires	0.71
Persian Gulf	Maskat	0.67
	Abushehr	1.14
Chinese Gulf	Pigumdo	0.39
	Taku	0.57
Baltic Sea	Korsør	0.17
	Copenhagen	0.29
	Gedser	0.77

The following considerations may perhaps also be of interest. We have found that on a rotating disc waves of the kind here considered, must have a period length shorter

than half the time used by the disc for one revolution. Using our previous notations, this is expressed by

$$\sigma > \lambda$$

or, introducing

$$\lambda = 2\omega \sin \varphi$$

$$\sigma > 2\omega \sin \varphi$$

If the theoretical results could be applied to the conditions on the rotating earth without any restrictions they would envolve that for each partial wave of period length T hours we could compute a maximum value of φ defined by

$$\sin \varphi = \frac{\sigma}{2\omega} = \frac{12}{T}$$

which would represent the greatest value of the geographic latitude, where the partial wave in question could exist. We should thus find

	φ_{max}
S_2	90°
M_2	75°
N_2	72°
K_1	30°
O_1	28°

It is, however, not permissible to conclude that diurnal tidal waves cannot possibly exist on a continental shelf north or south of a latitude of about 30°, because we always deal with limited regions on a rotating sphere. Nevertheless it seems worth while mentioning that all the large regions with diurnal tides are found in the equatorial zone, and that diurnal tides only exceptionally are met with in higher latitudes.

The preceding considerations are sufficient to show that complicated tidal phenomena may be expected on the continental shelves even when originating from a single wave. This is best illustrated by the tidal phenomena observed on the North Siberian shelf, to which we now shall return.

17. Applications to the tidal wave on the North Siberian shelf.

We have previously arrived to the result, that all tidal observations from the North Siberian shelf could be united into a consistent picture of a single wave, entering the shelf from the North, but representing a wave which has little in common with a long wave, proceeding in a non-viscous fluid in a resting basin. Attention was drawn to the main points on which the tidal wave on the North Siberian shelf differs from an ordinary long wave. We can now explain the characteristic features one by one as the combined results of the deflecting force and the resistance, modified by the coasts. We will, however, not enter upon the variations in the quality of the tide because the observations are insufficient for a discussion of these variations.

1. *The rotary character of the tidal currents.* A glance at Fig. 4 shows that the currents rotate clockwise within the whole region, but that the ratio between minimum and maximum current, indicated by the ratios of the axes of the ellipses, varies from practically zero north of the New-Siberian Islands, where the wave proceeds along the coast, to 0.8 or 0.9 in the regions where the distances to the coasts are great. This is in perfect agreement with the preceding results. Where no hindrances prevent the development of the rotary currents, these are dominating; where the wave proceeds along a coast,

the currents are alternating. Regarding the tidal currents off point Barrow Harris states, that the flood current, defined as the current whose maximum falls on the rising tide, sets towards east, and that the maximum according to observations taken by Collinson on July 25 and July 26, 1851, occurs 2.5 hours before highwater at the coast. He also quotes Simpson, who regarding the strength of the current writes: «I could not help remarking that the velocity of both ebb and flow (current) was far greater than the inconsiderable rise and fall would led me to expect». These observations are in agreement with the conception that the tidal wave approaches the coast from the north. According to Fig. 4 the conditions at point Barrow correspond to those illustrated in Fig. 10, p. 61. By the discussion of this example it was found that the transversal currents should be expected close to the coast and reach great velocities relative to the range.

Using $\varphi = 75^0$ as a mean value of the geographic latitude for the region and introducing $T = 12.4$ hours as the period length of the wave, we find:

$$s = 1.0 .$$

According to this the wave should be on the verge of degenerating and the currents should run with the same velocity in all directions. These conditions are actually approached, particularly in the region between Wrangell Island and Bennett Island where, for instance at station *2*, the ratio between minimum and maximum current was found to be 0.9.

2. *The variations of the tidal currents with depth.* The variations of the tidal currents with depth are very complicated. The tidal wave proceeds between two boundary surfaces of which the upper, the ice, offers no resistance to vertical displacements, but a considerable resistance to horizontal displacements. The latter varies with the seasons, being small in the summer, when lanes and spaces of open water give the ice a limited freedom of motion, and very large in winter, when every opening is immediately covered with new ice. Furthermore, the eddy viscosity is far from being constant, because the density varies with the depth. We shall here illustrate the most typical conditions by examples from the 3 stations at which the range of the tide and the tidal hour were determined practically simultaneously by soundings.

Station 8. At Station 8 (see Fig. 1, p. 5) the tidal currents were observed in two depths, 0 and 12 meters. The result of the harmonic analysis of the observations is given in Table 30, using the same quantities for representation as previously (see p. 19). The values for the mean current have been derived by assuming the currents 3 meters above the bottom, not measured at Station 8, to have the same character as at two adjacent stations. From the table it is seen that the velocity of the maximum current is practically unchanged in the upper 12 meters but occurs slightly earlier in 12 than in 0 meters. In 0 meters the currents are practically alternating, in 12 meters rotate clockwise, but the minimum current is weak.

Table 30. Tidal currents at Station 8; July 18, 1925, 9^h to 20^h. Lat. 76° 28′ N; Long. 141° 30′ E; Depth 22 m.

Depth. m.	Max. tidal current			Min. current	Min./Max.	Dir. of rotation
	Cm/sec.	Against true	Tidal hour			
0	41.5	S 50° E	3.1	1.0	0.02	c. cl.
12	42.5	S 44° E	2.8	10.5	0.25	cl.
Mean 0 – 12	38.0	S 45° E	3.0	5.0	0.13	cl.

Fig. 13 A contains a vertical section which has been laid NW — SE, in the direction in which the wave is supposed to proceed according to the cotidal lines in Fig. 4. The component of the current in the direction of progress is here represented for every Greenwich lunar hour. The curvature to the left of the lines indicates that the current turns at an earlier moment when approaching the bottom. Fig. 13 B contains two horizontal sections in which the currents in 0 and 12 meters have been represented by central vector diagrams.

Two circumstances show that the wave is meeting a great resistance; the maximum tidal current is reached about 2 hours before highwater (see Fig. 4), and the wave proceeds with a velocity of only 10 m/sec., but the formula $\sqrt{gh}$ gives with $h = 22$ m.

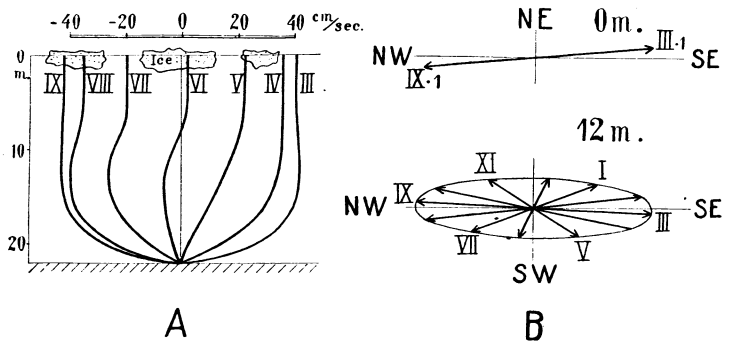

Fig. 13. Tidal currents at station 8, July 18, 1924.

14.7 m/sec. We may obtain an idea of the character of the resistance by comparing the observed currents with currents which may be computed from equations 3, Chapter 10, introducing simple assumptions. Since the currents are practically alternating we shall assume that the deflecting force can be left out of account, being balanced by a transversal slope of the wave crest. We shall, therefore, introduce

$$s = 0.$$

Furthermore, we will suppose the upper surface to be free, the velocities at the bottom to be zero, and the eddy viscosity to be constant. The value of the latter will be so selected that the computed velocity of progress agrees with that observed. The observed velocity is, expressed in fractions of $\sqrt{gh}$:

$$10 \text{ m/sec.} = 0.68 \sqrt{gh}\,.$$

We find, therefore, the value of η, which is to be used by entering Table 7, in the column $s = 0$ and to the left seek the value of βh, which corresponds to $c : c_0 = 0.68$. We find:

$$\beta h = 0.7$$

Introducing

$$\beta = \sqrt{\frac{\pi}{T\eta}} = \frac{1}{\sqrt{\eta}} \cdot 0.84.10^{-2} \quad \text{and} \quad h = 2200 \text{ cm.}$$

we get

$$\eta = 690 \text{ gr. cm.}^{-1} \text{ sec.}^{-1}.$$

Finally, we shall assume that highwater occurs at the observed time, 5 Gr. lunar hours, and choose the range such that the computed mean velocity of the currents agrees with the observed.

The result of the computation is represented graphically in Fig. 14 which corresponds to Fig. 13 A. In order to facilitate a comparison, the outline of the latter has been entered as a stippled line on Fig. 14. We find at first, that the computed currents reach a maximum velocity about 1.1 hours before highwater, but the correspondingly observed difference is 2 hours. This discrepancy can hardly be due to errors of observation, because a close inspection of all available data from this region resulted in no reduction in the observed difference in time. It appears that this only partly can be explained as an effect of the resistance, for which reason we shall return later to the subject. Continuing the comparison, we find, that the observed currents in the upper layers change more slowly with depth than those computed, but more rapidly close to the bottom. These features can be ascribed to:

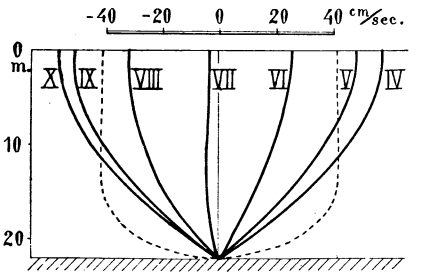

Fig. 14. Computed tidal currents.

1. That the ice offers a resistance which reduces the velocities of the upper layers.

2. That the eddy viscosity is smaller than assumed. This applies particularly to the layers above the bottom, where the velocities change rapidly.

The resistance thus seems to have another character than that assumed when computing the currents, but the differences can be accounted for. The variation of density with depth at this station showed no remarkable features.

Finally, we may assume that the damping of the wave takes place at the same rate as it would under the conditions upon which the computation of the currents were based, in spite of the different character of the resistance. From Table 6 we then find

$$p = 0.68$$

corresponding to $\beta h = 0.7$ and $s = 0$. By means of this value, the maximum velocity of the mean tidal current and the rate of progress of the wave the range of the tide can be computed by means of the formula (p. 42):

$$2\zeta = 2h\frac{\bar{u}}{c}\sqrt{1+p^2}$$

We find

$$2\zeta = 203 \text{ cm.}$$

which value accidentally agrees almost exactly with the observed range, 210 cm. No great weight can be attached to this agreement, but it shows that the various observations are in mutual concordance.

Station 7. At Station 7 the tidal currents were more complicated. In Table 3, p. 9, the mean tidal current according to observations on June 30 and July 3, 1924, has been entered, but we shall here deal with the observations from June 30 only, because these are most complete. The tidal currents on that day were determined at 4 depths, 0, 15, 23, and 31 meters; the depth to the bottom was 35 meters. The results of the harmonic analyses are contained in Table 31 and represented graphically in Fig. 15.

Table 31. Tidal currents at Station 7. June 30, 1924, $8^h\ 30^m$ to $21^h\ 30^m$. Lat. 76° 32′ N. Long. 144° 00′ E. Depth 35 m.

Depth m.	Max. tidal current			Min. tidal current cm/sec.	Min./Max.	Dir. of rotation
	Cm/sec.	Against (True)	Tidal hour			
0	16.2	S 5° W	4.2	7.0	0.43	cl.
15	15.2	S 29° E	3.9	9.0	0.59	cl.
23	14.8	S 30° E	5.4	6.5	0.44	cl.
31	10.1	S 30° E	4.9	0.0	0.00	—
0—35	12.4	S 14° E	4.4	4.5	0.37	cl.

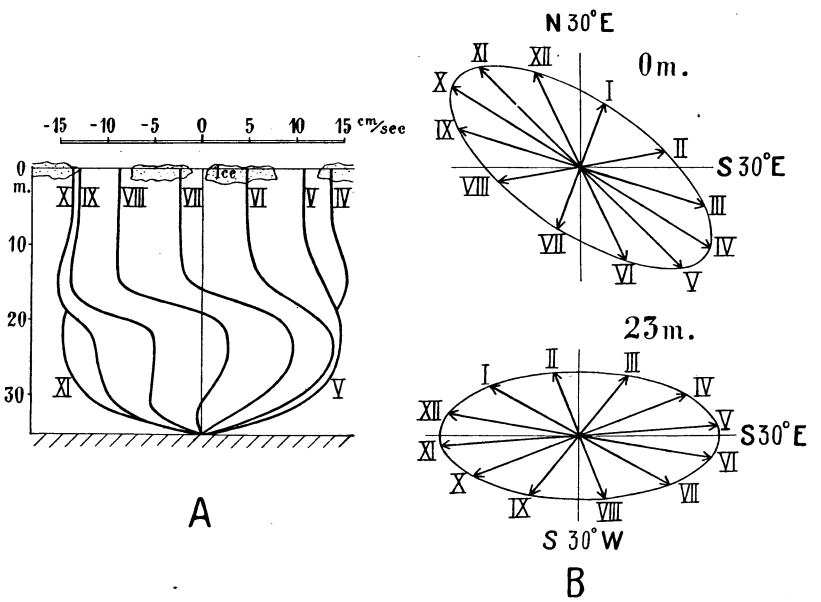

Fig. 15. A. St. 7. Vertical section showing component of tidal current in the supposed direction of progress of the wave.
Fig. 15. B. Horizontal sections showing tidal currents in 0 and 23 m.

The conditions at this station are too complicated to permit a computation of an approximately adequate example by means of the previously developed equations. The influence of the resistance, however, is plainly visible in the main features of the currents. The tidal hour at spring at this station is about 5.5 hours. A glance on the table shows that the maximum current occurs before highwater, both at the surface and close to the bottom, indicating the influence of the resistance. In Fig. 15 A this effect is visible in the double curvature to the left of the lines, representing the component of the current in the direction in which the wave is supposed to proceed, N 30° W to S 30° E. The direction of the maximum current at the surface deviates considerable to the right of the direction of progress, in which the combined influence of the resistance and the deflecting force are recognized. A corresponding deviation should be expected close to the bottom, but was not observed on that day. It might, furthermore, have been expected that the greatest velocities would have been found in the medium depths, but the fact that the velocities are relatively small seems to indicate that the eddy viscosity prevents the development of the velocities even at the greatest possible distances from the boundary

surfaces. The time difference between highwater and the mean maximum current at this station is not greater than that it can be referred to the influence of the resistance.

We may again compute the range of the tide by means of formula (36), Chapter 10, assuming that the exponent of damping at this station is somewhat smaller than at Station 8. Introducing the value of $\bar{u}$ derived from the observations on June 30 and July 3, $\bar{u} = 16\ 5$, furthermore $c = 12$ m/sec., $h = 35$ m., and $p = 0.6$, we find:

$$2\zeta = 112 \text{ cm.}$$

in fair agreement with the observed range of 92 cm.

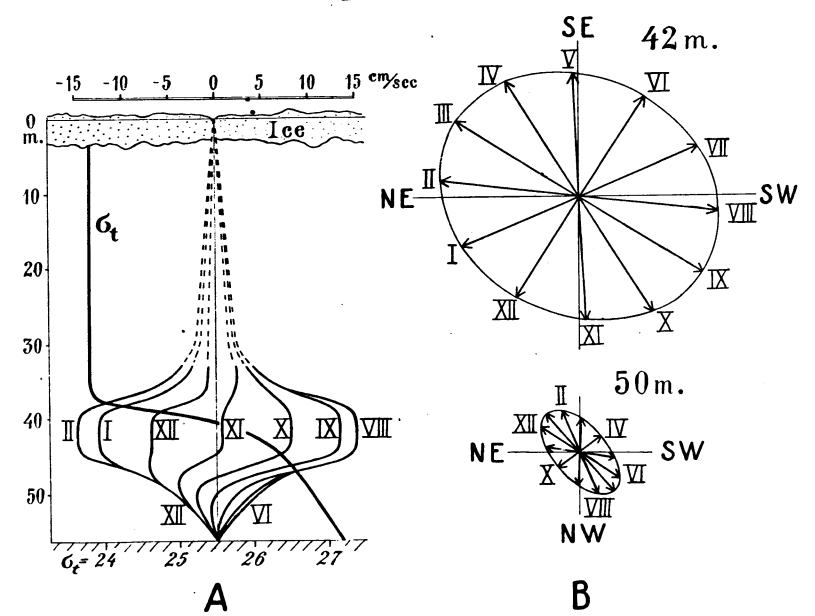

Fig. 16. A. St. 3. Vertical section showing component of tidal current in the supposed direction of progress of the wave.
Fig. 16. B. Horizontal sections showing tidal currents in 42 and 50 m.

Station 3. The results of the observations at this station were given in Table 4, p. 9, and are here represented graphically in Fig. 16, which clearly shows the peculiar character of the currents. The vertical section has been laid in the direction in which the wave proceeds according to the cotidal lines, NE — SW, and the two horizontal sections represent the currents in 42 meters and 50 meters respectively.

The ice at this station as ascertained by numerous measurements, took no part in the tidal movement, and the currents were too weak to be recorded in all depths down to 30 meters. This has been indicated by drawing the lines in Fig. 16 A as straight, stippled lines from the surface to 30 meters. From 35 to 40 meters the velocities of the currents increased rapidly, and between 40 and 45 meters strong tidal currents were encountered. Approaching the bottom, the velocities again decreased, though more slowly, and simultaneously the maximum current occurred at an earlier time and was directed to the right, referred to the corresponding direction in 42 meters. We recognize the well-known influence of the resistance along the bottom, transferred by the eddy viscosity to considerable distances.

The variation of the density with depth gives the clue to the understanding of these tidal currents. The heavy curve in Fig. 16 A represents σ_t as function of the depth. It is seen that the density is constant from the surface and down to a depth of about 37 meters, increases very rapidly between 37 and 42 meters, less rapidly from 42

to 48 meters, and finally, comparatively slowly from 48 meters to the bottom in 56 meters. According to this variation the upper layer is practically in indifferent equilibrium, the stability is here very small. In the middle-layer, on the other hand, the stability is very large, but decreases from 42 meters towards the bottom. The eddy-viscosity, as previously mentioned (p. 28), must be expected to be approximately inversely proportional to the stability. In the upper layer the eddy viscosity must be very great, in the middle layer very small, and in the bottom layer again considerable. As a rough approximation the wave can be regarded as proceeding between two boundary surfaces, of which the upper offers no resistance to vertical displacements, and in a fluid consisting of 3 layers of slightly different densities, such that no exchange of mass takes place between these layers. We have previously (Chapter 13) developed the equations for the currents in this case, and have there computed an numeric example, Table 27, selecting the numerical values to suit the conditions at the station, with which we now are dealing. The fluid at that time was devided into 3 layers of the relative thicknesses

$$h_1 = 0{,}665\ h \quad , \quad h_2 = 0.09\ h \quad , \quad h_3 = 0.245\ h$$

where h means the depth which is now equal to 56 meters, and where the index 1 refers to the upper layer. These thicknesses were selected to represent the layers that we here have called the upper, the middle, and the bottom layer. The value of s was supposed to be 0.9. The eddy viscosities in the upper and the bottom layers should satisfy the equations

$$(\beta h)_1 = 1.0 \quad , \quad (\beta h)_3 = 3\,0.$$

Introducing the expression for β, and $T = 12.4$ hours, $h = 56$ meters, we find in the present case

$$\eta_1 = 980 \text{ g.cm.}^{-1} \text{ sec.}^{-1} \quad , \quad \eta_3 = 14.7 \text{ g.cm.}^{-1} \text{ sec.}^{-1}.$$

The eddy viscosity of the middle layer is of no importance under the supposed conditions. The above values of η were introduced in order to:

1. Reduce the computed velocities in the upper layer so far that they would be too small to be observed.

2. Make the computed velocity of progress agree with that observed. The latter is 27 m/sec. As computed value we found $c = \sqrt{gh} \cdot 1.20$ which with $h = 56$ m. gives

$$c = 28\,1 \text{ m/sec.}$$

We shall now, furthermore, make the computed velocity in 42 meters agree with that observed, and as time for highwater introduce the observed tidal hour 8^h.

It may seem that so many assumptions have been made that the computed currents must agree with those observed. The point is, however, that it is possible to assume such values, particularly of the eddy viscosity, that it is possible to compute currents which approximately agree with those observed, because this enables us to understand the character of the eddy viscosity.

The computed currents have been represented in Fig. 17 in the same scale as those observed, and to facilitate the comparison the outline of Fig. 16 A and the density curve have been entered as stippled lines. There is evidently a great similarity between the computed and the observed currents. The general characters of the curves in the vertical section, representing the component in the supposed direction of progress, is the same, and comparing the horizontal sections, we find in both cases that the currents in 42 meters attain a maximum velocity before highwater, but in 50 m. after highwater, that the direction of the latter is turned to the right referred to the corresponding direction

in 42 meter, and that the ratio between minimum and maximum current decreases from 42 to 50 meters. According to the observations, even the maximum current in 42 meters is turned to the right referred to the direction of progress, perhaps indicating that the wave proceeds in a more westerly direction than supposed. A more westerly direction of progress can, however, hardly be brought in concordance with the course of the cotidal lines. Another discrepancy, which is not evident from the figures but from Table 4, is that the observed direction of maximum current in 46 meters does not fall between the corresponding directions in 42 and 50 meters, but to the left of both of them.

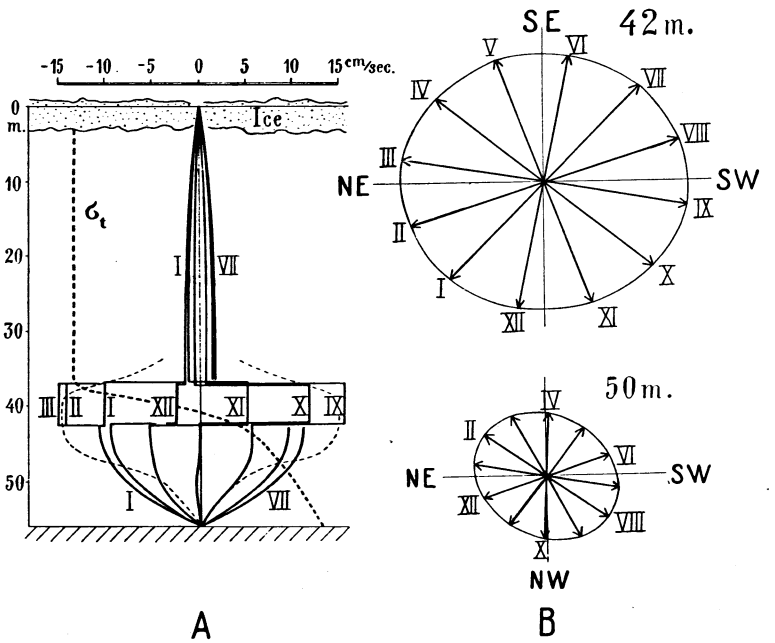

Fig. 17. A. Vertical section showing component of computed tidal currents in the direction of progress.
Fig. 17. B. Horizontal sections showing computed tidal currents in 42 and 50 m.

Turning again to Figures 16 A and 17 A, we may at first draw attention to the phase difference between the observed and computed currents. In Fig. 16 A the curve farthest to the right is marked VIII, in Fig. 17 A marked IX. This phase difference would dissapear if the wave had been assumed to proceed towards S 70° W, but this does not appear to be permissible.

The greatest and most interesting discrepancy between the observed and the computed currents, is the difference in the rate with which they change with depth. We do not know anything about the character of the tidal currents in the upper layer, because they were too weak to be observed, but the very fact that they were so weak is evidence that the eddy viscosity actually had a value of the assumed order of magnitude, about 1000 c.g.s. The very rapid increase in the currents between 35 and 40 meters is in close agreement with the supposed condition, showing that the eddy-viscosity in this depth must be small. This is confirmed by the sharp bend of the density-curve between 37 and 38 meters. The great velocities observed in 46 meters indicate, on the other hand, that the eddy-viscosity is not zero at the boundary between the middle and the bottom layer. This boundary is actually very undefined; the density curve is smoothly curved, showing a continuous transition. Close to the bottom the computed current decreases more rapidly than that computed, indicating that the eddy viscosity here has a considerably higher value than 14.7, which was assumed for the whole bottom layer.

Generally, the variations of the currents with depth must be regarded as in good agreement with the supposed character of the eddy-viscosity, the differences being accounted for by the circumstance that the density changes continuously, and not, as supposed, discontinuously.

The exponent of damping at this station was under the supposed conditions found to be (p. 51) $p = 0.35$. Introducing this value, $\bar{u} = 3.8$ cm/sec., $c = 27$ m/sec., and $h = 56$ m. in equation (36), Chapter 10, we find the range

$$2\zeta = 17 \text{ cm.}$$

in excellent agreement with the observed range of 18 cm.

Finally, we may compare the values of the eddy-viscosity which have been introduced here with the values which previously have been derived mainly from the change of the drift-currents with depth. (Compare p. 27). Ekman(1) has found a value of η of about 200, Krümmel finds in an example $\eta = 297$ and 237(2), and W. Schmidt(3) adopts $\eta = 100$ as an average value for the sea. The values here used are respectively

$$\eta = 690 \quad , \quad \eta = 14.6 \quad \text{and} \quad \eta = 980 \text{ gr. cm.}^{-1} \text{ sec.}^{-1}$$

but the first was found to be too large and the second too small. The third was found approximately correct, but in a layer in indifferent equilibrium, representing extreme conditions. Considering these circumstances, the values here introduced of the eddy viscosity must be regarded as in fair agreement with the previous ones which were derived in entirely different ways.

3. *Discrepancy between time of highwater and time of maximum current.* On p. 14 attention was drawn to the circumstance that the maximum tidal currents north of the New-Siberian Islands appears to be reached a considerable time before highwater. In the preceding section it was shown, that this time difference can partly be explained as the effect of the resistance, but that it seems too great to be entirely the result of the latter. If, however, we compare the picture of the tidal wave in this region (Fig. 4) with the formal example in Fig. 11, we find a striking similarity. In the discussion of this example we came to the result, that when a wave runs along a coast lying on the right hand, highwater must occur after the maximum current. The observed conditions seem to illustrate this example.

4. *The rate of progress.* From Fig. 4, it will be seen that the wave proceeds with a great velocity where the currents are rotating, and with a small velocity where they are practically alternating, in agreement with the conclusions in the preceding chapter.

We may compare the observed velocities of progress with these computed from the equation (p. 24):

$$c = \sqrt{gh}\sqrt{\frac{1 - r^2}{(1 - sr)^2}}$$

This equation should be approximately correct if the wave met no resistance, but as we have seen that this condition is not fulfilled, we must expect the observed velocities to be smaller. We select 4 representative stations, of which the two first are situated north of the New-Siberian Islands, and the two last west and east of Wrangell Island respectively. At the last station, the actual depth was 76 meters, but as this value represents

(1) On the influence of the earth's rotation etc. Arkiv för mat., astr. och fysik V. 2. No. 11.

(2) L. c. p. 461. The values there given are 10 times smaller, probably on account of an error in calculation.

(3) Der Verbrauch an Strömungsenergie im Meere. Ann. d. Hydr. u. Mar. Met. XLVII, 1919, p. 11.

a local indentation we shall introduce the value 60 meters, which is in better agreement with the average depth of the surroundings (see Fig. 4). In Table 32, the computed and observed velocities of progress are compiled.

Table 32.

St. No.	Depth m.	s	r	$\sqrt{gh}$	c comp. m/sec	c obsv. m/sec.
8	22	1.0	0.1	14.7	16.2	10
7	35	1.0	0.3	18.5	25.1	12
3	56	1.0	0.8	23.4	70.1	27
1	60	1.0	0.8	24.2	72 5	65

The observed velocities are at all station smaller than those computed, at the two first where the currents are approximately alternating, even smaller than $\sqrt{gh}$, but at the last two greater than $\sqrt{gh}$.

The difference between Stations 1 and 3, east and west of Wrangell Island, is remarkably great. We have seen that the peculiar tidal currents at Station 3 were the result of the character of the eddy viscosity, which again was explained by the hydrographic conditions at this station. The same applies to the velocity of progress. The wave proceeds actually as if the upper layer did not exist, and the wave were proceeding in a sea with a depth of 16 meters only and not 56 meters (p. 51). This clearly shows the importance of the hydrographical conditions, in this case the stratification of the water, for the velocity of progress. The difference in this velocity east and west of Wrangell Island may therefore be due to different hydrographical conditions within the two regions. The oceanographical observations from August and September, 1922, at stations east of Wrangell Island confirm this view in so far, as no stratification was found there. This may be due to the season, but the oceanographical observations from the region northwest of Wrangell Island, on the other hand, show that the conditions, which were illustrated by the density curve at Station 3, prevail there through the whole year. More extensive observations, however, are required from the region east of Wrangell Island, in order to examine the value of the suggested explanation.

5. *The variation of the range of the tide.* Attention has previously been drawn to the fact, that the range of the tide varies both along the cotidal lines, and in the direction of progress. In the following we shall disregard the range observed at Cape Chelyuskin, because on account of the divergent character of the tidal wave in the Nordenskiöld Sea this cannot be brought directly in connection with the other ranges. We then find, that the range generally decreases from west to east at the most northerly stations, or referred to the direction of progress from right to left, in agreement with the conclusions on page 61. Arranging these stations according to longitude, we find:

Station	8	7	Bennett Isl.	3	Point Barrow
Longitude	141.5	144,0	149	166.2 E. Gr.	156°.7 W. Gr.
Range, cm.	210	92	105	18	14

The decrease is evidently more rapid off the New-Siberian Islands where the currents are alternating, than further east where they are rotary, again in agreement with our conclusions.

Supposing that the range in the region where the currents are alternating decrease approximately according to the law

$$\zeta = \zeta_0 e^{-\frac{\lambda}{c} y}$$

(p. 20) we can compute the ranges at St. 7 and at Bennett Island from the range observed at Station 8. We find, introducing $\lambda = 2\omega \sin 76° = 1.32.10^{-4}$:

	St. 7	Bennett Isl.
y = Distance from Station 8 along cotidal lines	50.10^3 m	150.10^3 m.
Mean c	10 m/sec.	12 m/sec.
Computed range, cm.	108	41
Observed range, cm.	92	105

According to this the observed range at Station 7 is in good agreement with the supposed conditions, but the range at Bennett Island is considerably too great. This may be due to local convergence caused by the Island. The decrease from right to left, however, mainly seems to be the effect of the rotation of the earth.

The decrease in the direction of progress, on the other hand, is due to the resistance. In the region north of Ajon Island and Bear Islands the wave seems to proceed with an almost straight front, and it should, therefore, be possible to compute approximately the values of the coefficient of damping, p, by means of the observed ranges at Station 3, Ajon Island and Bear Islands, using the formula

$$\zeta = \zeta_0 e^{-\gamma x} = \zeta_0 e^{-p \frac{2\pi}{L} x}$$

We assume, however, by adopting this equation, that the currents off the coast have the same character as at Station 3, and since information is lacking, we cannot expect to find very reliable results.

In the above equation we can conveniently introduce

$$\frac{t}{T'} = \frac{x}{L}$$

where t means the difference in lunar hours between the time of highwater at the stations and T' the period length in lunar hours, viz. 12 hours. We then find from Stations 3 and Ajon Island

$$18 \cdot e^{-p \cdot 2\pi \cdot \frac{1}{12}} = 5 \quad ; \quad p = 0.62$$

and from Stations 3 and Bear Islands:

$$18 \cdot e^{-p\, 2\pi \cdot \frac{1}{12}} = 3 \quad ; \quad p = 0.54.$$

Both values are in fair agreement with the value $p = 0.35$, which was found from the current observations at Station 3, far off the coast.

Observations of the range of the tide and the tidal hours along the northern coast of the New-Siberian Islands would have been of great interest, because on account of the course of the cotidal lines and the shallow water we may there expect rapid changes, but such observations are still lacking.

In the preceding section the importance of the hydrographical conditions for the velocity of progress was mentioned. We might also have there included the importance of the resistance offered by the ice. Both these factors are evidently of importance for the damping of the wave. Considering this, numerous variations of tidal hours and ranges along the Siberian coast must be expected. Particularly a yearly period in tidal hour and range seems probable, because the resistance of the ice has a marked yearly period, and in addition the sea off the coast is generally more or less free of ice in the summer. The available observations, however, are from too limited periods to permit a study of these relations.

Summing up the results of the preceding discussion, it seems justifiable to say that the tidal phenomena on the North-Siberian shelf on every point confirm the results of the theoretical investigations which, on the other hand, were suggested by the observation of these phenomena.